TECTONICS, VOL. 29, TC3005, doi:10.1029/2009TC002449, 2010

Influence of climate change and uplift on Colorado Plateau paleotemperatures from carbonate clumped isotope thermometry

K. W. Huntington,[1] B. P. Wernicke,[2] and J. M. Eiler[2]

Received 21 January 2009; revised 17 August 2009; accepted 28 December 2009; published 25 May 2010.

[1] The elevation history of Earth's surface is key to understanding the geodynamic processes responsible for the rise of plateaus. We investigate the timing of Colorado Plateau uplift by estimating depositional temperatures of Tertiary lake sediments that blanket the plateau interior and adjacent lowlands using carbonate clumped isotope paleothermometry (a measure of the temperature-dependent enrichment of ^{13}C-^{18}O bonds in carbonates). Comparison of modern and ancient samples deposited near sea level provides an opportunity to quantify the influence of climate and therefore assess the contribution of changes in elevation to the variations of surface temperature on the plateau. Analysis of modern lake calcite from 350 to 3300 m elevation in the southwestern United States reveals a lake water carbonate temperature (LCT) lapse rate of 4.2 ± 0.6°C/km. Analysis of Miocene deposits from 88 to 1900 m elevation in the Colorado River drainage suggests that the ancient LCT lapse rate was 4.1 ± 0.7°C/km, and temperatures were 7.7 ± 2.0°C warmer at any one elevation than predicted by the modern trend. The inferred cooling is plausible in light of Pliocene temperature estimates off the coast of California, and the consistency of lapse rates through time supports the interpretation that there has been little or no elevation change for any of the samples since 6 Ma. Together with previous paleorelief estimates from apatite (U-Th)/He data from the Grand Canyon, our results suggest most or all of the plateau's lithospheric buoyancy was acquired ~80–60 Ma and do not support explanations that ascribe most plateau uplift to Oligocene or younger disposal of either the Farallon or North American mantle lithosphere.

Citation: Huntington, K. W., B. P. Wernicke, and J. M. Eiler (2010), Influence of climate change and uplift on Colorado Plateau paleotemperatures from carbonate clumped isotope thermometry, *Tectonics*, *29*, TC3005, doi:10.1029/2009TC002449.

1. Introduction

[2] Topography is a first-order expression of the buoyancy of the lithosphere, and thus the timing and pattern of elevation change can provide fundamental constraints on problems in continental dynamics. Topography also strongly influences circulation of the atmosphere and global climate [e.g., *Manabe and Terpstra*, 1974; *Ruddiman and Kutzbach*, 1989; *Molnar and England*, 1990; *Molnar et al.*, 1993]. Although technological advances allow us to measure modern elevation with unprecedented precision, paleoelevation remains difficult to reconstruct from the geologic record. For many of the most frequently used proxies for paleoelevation, this difficulty arises because changes in climate and changes in elevation can have the same effect on the proxy.

[3] The most commonly applied techniques for reconstructing paleoelevation are based on paleobotany or the stable isotopic record of meteoric and surface waters preserved in authigenic and pedogenic minerals [e.g., *Forest et al.*, 1999; *Chamberlain and Poage*, 2000]. Plant assemblages and leaf physiognomy vary with the combination of temperature, aridity, and enthalpy, from which elevation may be inferred [*Axelrod*, 1966; *Gregory and Chase*, 1992; *Wolfe et al.*, 1997; *Forest et al.*, 1999]. Meteoric and surface waters generally decrease in $\delta^{18}O$ and δD with increasing altitude. However, isotopic gradients also depend on aridity, temperature, and seasonality of precipitation [e.g., *Dansgaard*, 1964; *Garzione et al.*, 2000; *Rowley and Garzione*, 2007], and temperature decrease accompanying uplift dampens isotopic evidence of elevation change recorded by carbonates on uplifted topographic features [*Poage and Chamberlain*, 2001]. Given the many factors that contribute to the character of flora and isotopic signals preserved in the geologic record, the accuracy of resulting paleoelevation estimates is often difficult to assess. The new carbonate clumped isotope paleothermometer [*Ghosh et al.*, 2006a; *Eiler*, 2007] provides independent constraints on both the temperature and isotopic composition of ancient surface waters, offering a potentially powerful approach to reconstruct past elevations [*Ghosh et al.*, 2006b; *Quade et al.*, 2007].

[4] In this paper, we investigate the timing of Colorado Plateau uplift by comparing measurements of both modern and ancient depositional temperatures of lake sediments that blanket the plateau interior and adjacent lowlands. To our knowledge, this is the first comprehensive analysis of how recorded carbonate clumped isotope temperatures vary with elevation in modern lakes. In addition, we compare modern and ancient samples deposited near sea level in order to

[1]Department of Earth and Space Sciences, University of Washington, Seattle, Washington, USA.
[2]Division of Earth and Planetary Sciences, California Institute of Technology, Pasadena, California, USA.

0278-7407/10/2009TC002449

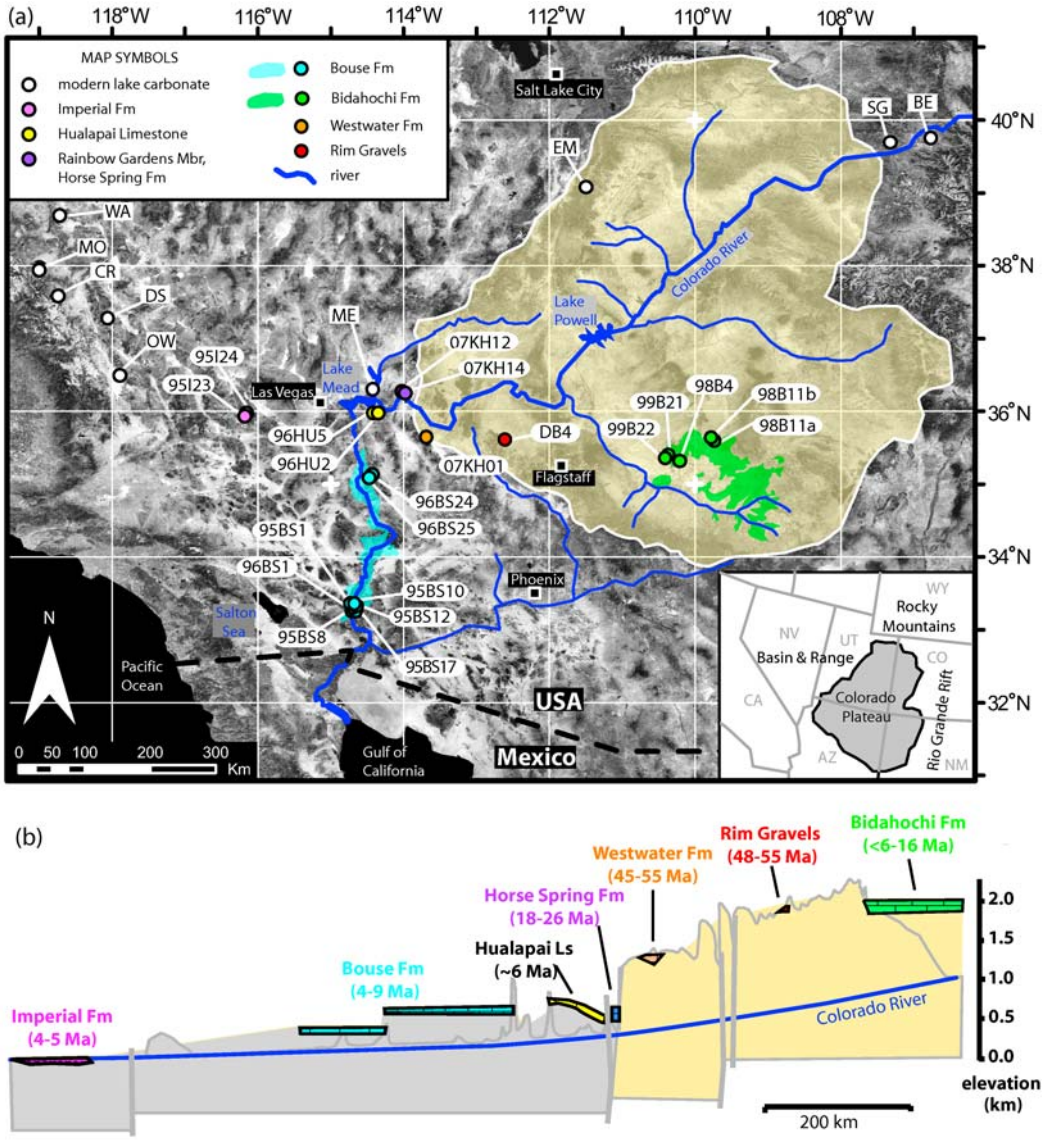

Figure 1. (a) Satellite image of western United States showing carbonate sample locations in relation to map extent of Colorado Plateau (tan shaded region). Inset shows relation of Colorado Plateau to state boundaries and neighboring tectonic provinces. The areas shaded green and blue delimit the extent of land containing discontinuous outcrops of the Bidahochi and Bouse formations, respectively. Labels for modern lake carbonate samples correspond to abbreviations listed in Table 2. (b) Relative elevations of sampled units are shown projected onto a schematic longitudinal profile of Colorado River. Locations of faults (subvertical thick gray lines) are from *Karlstrom et al.* [2007]. The inferred position of the Imperial Formation (tidal flat facies) indicates deposition at sea level near present mouth of the Colorado River into the Gulf of California.

quantify the influence of climate change on observed temperature signals.

2. Tectonic Setting of the Colorado Plateau and Previous Paleoaltimetry

2.1. Mechanisms Driving Plateau Uplift and Existing Paleoelevation Constraints

[5] The Colorado Plateau is a 2 km high, roughly 337,000 km^2 physiographic region bounded by the Rocky Mountains, Rio Grande Rift, and Basin and Range provinces in the southwestern United States (Figure 1). A wide variety of geodynamic hypotheses for uplift have been advanced wherein the timing of uplift is among the most testable predictions [e.g., *McGetchin et al.*, 1980; *Morgan and Swanberg*, 1985]. A summary of mechanisms broadly ascribes them to three categories [*Roy et al.*, 2005]: (1) late Cretaceous to early Tertiary uplift related to Sevier and Laramide contractile deformation from 80 to ~40 Ma, adding buoyancy by thickening of the crust, thinning of the

upper mantle, or the introduction of volatiles to the upper mantle [e.g., *Bird*, 1979; *McQuarrie and Chase*, 2000; *Humphreys et al.*, 2003]; (2) mid-Tertiary uplift related to the demise of a Laramide flat slab, where buoyancy is added to the upper mantle by mechanical thinning or chemical modification of the lithosphere [*Spencer*, 1996; *Roy et al.*, 2005]; and (3) late Tertiary "epeirogenic" uplift associated with regional extensional tectonism, either by convective removal of lithosphere or heating from below [e.g., *Bird*, 1979; *Thompson and Zoback*, 1979; *Humphreys*, 1995; *Parsons and McCarthy*, 1995; *Jones et al.*, 2004; *Zandt et al.*, 2004]. Quantitative constraints on the timing of uplift therefore have the potential to falsify one or more of these hypotheses.

[6] Previous paleoaltimetry work in the western United States has focused on the Rocky Mountains and Basin and Range provinces, with a dearth of estimates from the Colorado Plateau. Estimates based on paleobotany suggest that regional surface elevations of the western United States were high in late Eocene time [e.g., *Wolfe et al.*, 1998; *Gregory and Chase*, 1992]. Stable isotope data generally support the idea of high elevation in the Sierra Nevada and Rocky Mountains throughout the Tertiary period [e.g., *Chamberlain and Poage*, 2000; *Dettman and Lohmann*, 2000; *Poage and Chamberlain*, 2002; *Horton et al.*, 2004; *Horton and Chamberlain*, 2006; *Mulch et al.*, 2006, 2007, 2008].

[7] An exception to this overall picture, which to our knowledge includes the only published paleoaltimetry data from the plateau proper, comes from basalt vesicle studies that suggest a general acceleration of uplift in late Tertiary time [*Sahagian et al.*, 2002]. These data indicate as much as 1100 m of uplift of the southern part of the plateau since just 2 Ma, although this conclusion is controversial [*Libarkin and Chase*, 2003; *Sahagian et al.*, 2003]. In contrast, along the southwestern margin of the plateau, ~1200 m of relief observed within Laramide paleochannels indicates at least that amount of elevation above sea level in early Tertiary time [*Young*, 2001]. Roughly 60 km to the northwest in the plateau interior, (U-Th)/He data suggest that a "proto-Grand Canyon" with kilometer-scale relief had incised post-Paleozoic strata in earliest Tertiary time [*Flowers et al.*, 2008].

2.2. Geology and Relevant Sedimentary Deposits

[8] The Colorado Plateau (Figure 1) lies in the foreland of the Cordilleran orogen in the southwestern United States, and has experienced relatively little tectonism in Phanerozoic time. In contrast, neighboring regions suffered profound deformation during late Paleozoic "Ancestral Rockies" orogenesis, the Late Cretaceous/early Tertiary Sevier and Laramide orogenies, and late Tertiary extension in the Basin and Range province and Rio Grande rift. Today, this tectonically stable physiographic region is drained by the Colorado River from its headwaters in the Rocky Mountains southwestward to the Gulf of California (Figure 1). In this paper, we designate the "upper basin" of the Colorado River as the high-elevation portion of the drainage, which is largely confined to the Colorado Plateau. We refer to the portion of the drainage within the lowlands to the southwest of the plateau, in the Basin and Range province, as the "lower basin," comprising the Lake Mead area and the Colorado River trough along the Arizona-California border.

[9] The beginning and end points of the Colorado Plateau's uplift are well known: the region remained near sea level until at least the late Campanian in Utah (~70 Ma) and the Turonian in Arizona (~90 Ma), and has been uplifted to a present average elevation of 1900 m. Constraints on the elevation of the plateau surface in the interval between these endpoints are sparse and controversial, prompting over a century of debate regarding how uplift of this deeply incised region was achieved without significant internal deformation of the upper crust [e.g., *Pederson et al.*, 2002; *Poulson and John*, 2003].

[10] The sedimentary record in the region provides a broad sampling of ages and positions of carbonate-bearing strata within the modern Colorado River basin and provides important constraints on erosion, tilting, and drainage adjustment on the plateau since Cretaceous time (Figure 1). Colorado River incision has exposed Proterozoic basement and overlying stratified rocks, capped by flat-lying Paleozoic to Mesozoic platform sediments [*Beus and Billingsley*, 1989; *Hintze*, 1993] that record slow subsidence and deposition during the platform's 500 My residence near sea level [*Hunt*, 1956]. Marine deposits in Arizona and Utah record the encroachment of the Cretaceous interior seaway, which covered most of the plateau [*Nations*, 1989]. Paleogene deposits along the western, northern, and eastern flanks of the plateau are up to several thousand meters thick [e.g., *Hintze*, 1993]. Age-equivalent strata known as the "Rim Gravels" are preserved along the southwestern margin of the plateau, recording early Tertiary unroofing and northeastward fluvial transport away from Laramide uplands to the southwest [*Young*, 1989; *Potochnik*, 1989, 2001]. In some exposures, Rim Gravels are preserved within deeply incised paleocanyons of the western Grand Canyon region, along with the ~45–55 Ma fluviolacustrine Westwater Formation [*Young*, 1999].

[11] Immediately southwest of the plateau, a broad region of Precambrian crystalline rocks is overlain unconformably by either Late Cretaceous or mid- to late Tertiary volcanic and sedimentary strata [e.g., *Hunt*, 1956; *Potochnik*, 2001]. Sevier- and Laramide-age (40–80 Ma) deposits around the northern and eastern perimeter of the plateau are overlain by extensive tracts of Oligocene to Recent volcanic rocks, while toward the center of the plateau they are intruded by small, isolated mid-Tertiary plutons. Along the plateau's southwest margin, Oligocene and younger volcanic and sedimentary deposits record a reversal of drainage from the northeast flowing streams draining Laramide uplands. After ~20 Ma, southwest flowing drainage was established, presumably induced by mid-Tertiary crustal extension and resulting loss of elevation within the former Laramide uplands relative to the plateau [*Peirce et al.*, 1979; *Young*, 1989; *Elston and Young*, 1991].

[12] Within the upper basin of the Colorado River drainage in northeastern Arizona, the Miocene Bidahochi Formation (Figure 1) presently resides at a relatively uniform

elevation of 1900 m above sea level, about the average elevation of the modern plateau. The thin, flat-lying deposits of the Bidahochi Formation record as much as 200 m of fluvial and lacustrine aggradation in a large internally drained basin that at maximum extent may have been greater than 30,000 km^2 in area [*Repenning and Irwin*, 1954; *Love*, 1989; *Dallegge et al.*, 2001; *Gross et al.*, 2001]. Isolated fossils and $^{40}Ar/^{39}Ar$ dating of volcanic ash beds derived from the Bidahochi basin and surrounding area indicate that sedimentation initiated at ~16 Ma and occurred episodically until 6 Ma [*Dallegge*, 1999; *Gross et al.*, 2001]. Outcrops of the Bidahochi Formation lie within 100 km to the east of the region of early Tertiary high relief (eastern Grand Canyon) described by *Flowers et al.* [2008]. As the Bidahochi Formation has never been substantially buried or deformed and covers a large region of the southern plateau interior, determining its paleoelevation would provide an important constraint on the uplift history, testing various hypotheses for the origin of the uplift.

[13] Within the lower basin, upper Miocene limestones currently at elevations ranging from 88 to 646 m were deposited in a chain of lakes that ultimately linked together to form the modern Colorado River between 5 and 6 Ma [*Spencer and Patchett*, 1997; *Spencer et al.*, 2008a; *House et al.*, 2008]. Immediately west of the plateau where the Colorado River enters Lake Mead, lacustrine sedimentation occurred both before and after a major pulse of mid-Miocene extension, including the Rainbow Gardens Member of the Horse Spring Formation (24 to 16 Ma) and the Hualapai Limestone (11 to 6 Ma), respectively (Figure 1) [*Faulds et al.*, 2001; *Spencer et al.*, 2001; *Lamb et al.*, 2005].

[14] Further to the south in the modern Colorado River trough, discontinuous exposures of the upper Miocene to lower Pliocene Bouse Formation record lacustrine aggradation in lakes developed just prior to the integration of the upper and lower basins (Figure 1). The southernmost of these basins, the Blythe basin, was about 100 km wide at its maximum fill level, and contains abundant marine fossils [e.g., *McDougall*, 2008]. Some workers have suggested these fossils were introduced into a wholly lacustrine setting by avian transport [*Dillon and Ehlig*, 1993; *Spencer and Patchett*, 1997; *Spencer et al.*, 2008b]. Whether the basin is lacustrine, marine or estuarine, it was likely near sea level and relatively close to an ocean at 5–6 Ma. The contemporaneous Imperial Formation records progradation of the Colorado River delta into the opening Gulf of California and Salton trough during early rifting and displacement along the San Andreas Fault [*Johnson et al.*, 1983; *Winker*, 1987; *Kerr and Kidwell*, 1991]. Detritus originating from the upper basin first appears in the Imperial Formation at 5.3 Ma [*Dorsey et al.*, 2007].

3. Paleoaltimetry Reconstructions From Carbonate Clumped Isotope Thermometry

3.1. Estimating Temperature and $\delta^{18}O$ of Water From ^{13}C-^{18}O Bond Enrichment in Carbonate

[15] Carbonate clumped isotope thermometry constrains carbonate growth temperatures based on the temperature-dependent "clumping" of ^{13}C and ^{18}O into bonds with each other in the solid carbonate phase alone, independent of the $\delta^{18}O$ of the waters from which the mineral grew [e.g., *Schauble et al.*, 2006; *Eiler*, 2007]. The ^{13}C-^{18}O bond enrichment relative to the "stochastic," or random, distribution of all C and O isotopes among all possible isotopologues can be determined by digesting a carbonate mineral in phosphoric acid and measuring the $\delta^{18}O$, $\delta^{13}C$, and abundance of mass-47 isotopologues (mostly $^{13}C^{18}O^{16}O$) in product CO_2. This enrichment, termed the Δ_{47} value, varies with carbonate growth temperature by the relation $\Delta_{47} = 59200/T^2 - 0.02$, where Δ_{47} is in units of per mil and T is temperature in Kelvin [*Ghosh et al.*, 2006a].

[16] Previous stable isotope paleoaltimetry studies have used the $\delta^{18}O$ and δD values of authigenic or metamorphic minerals to obtain information on past surface temperatures and surface waters, and thereby infer the paleoelevation of Earth's surface [e.g., *Chamberlain and Poage*, 2000]. However, the $\delta^{18}O$ of carbonate depends on both its formation temperature and the $\delta^{18}O$ of water from which it grew (i.e., through the temperature-dependent carbonate/water fractionation [e.g., *Kim and O'Neil*, 1997]). Thus, this conventional approach amounts to solving for two unknowns (T and $\delta^{18}O$ of water) with a single constraint ($\delta^{18}O$ of carbonate). Carbonate clumped isotope thermometry directly constrains both temperature and $\delta^{18}O$ of carbonate independently. From these values, the $\delta^{18}O$ of water from which carbonate grew can be calculated. Because both temperature and the $\delta^{18}O$ of water can vary strongly with elevation, this approach can provide two independent constraints on paleoelevation [*Ghosh et al.*, 2006b; *Quade et al.*, 2007].

3.2. Use of Temperature Lapse Rates to Infer Paleoelevation

[17] The $\delta^{18}O$ values of surface waters reflect surface and groundwater transport and evaporation in addition to the $\delta^{18}O$ of precipitation. As evaporation of water leads to ^{18}O enrichment in the residual liquid, the $\delta^{18}O$ values of surface waters do not correlate well with elevation in arid regions like the southwestern United States [e.g., *Rowley and Garzione*, 2007]. Rather, in the Colorado River drainage surface water $\delta^{18}O$ values plot below the global meteoric water line along an evaporation trend [*Guay et al.*, 2006].

[18] In contrast, modern air temperatures in this region do vary strongly with altitude. The rate of decrease of temperature with elevation based on mean annual air temperatures measured near the ground surface (MAT lapse rate) varies between 6.8 and 8.1°C/km throughout the Colorado Plateau region in Colorado, Arizona, New Mexico, and Utah [*Meyer*, 1992]. Based on this modern signal, we might expect environmental temperatures recorded by geologic materials formed at Earth's surface to be good indicators of relative elevation in the past. Estimates of MAT from paleoflora have been the basis for previous paleoelevation reconstructions [e.g., *Wolfe and Hopkins*, 1967; *Mosbrugger*, 1999]. In order to avoid complications arising from latitudinal variations in lapse rate, seasonality, and climate

Table 1. Summary of Clumped Isotope Thermometry and Stable Isotopic Results for Ancient Carbonates[a]

Sample[b]	$\delta^{13}C_{PDB}$ (‰)	$\delta^{18}O_{PDB}$ (‰)	$\delta^{18}O_{SMOW}$ (‰)	Analytical Δ_{47} (‰)	Analytical 1 SE Δ_{47} (‰)	1 SE Δ_{47} (‰)	Summary Average Δ_{47} (‰)	Summary Temperature ±1 SE (°C)
Imperial Formation (4–5 Ma)								
95-I-23	−1.8	−5.1	−0.3	0.593	0.0083	0.0131	0.588 ± 0.004	38.9 ± 1.7
	−1.9	−5.1	−0.2	0.591	0.0081	0.0111		
	−1.9	−5.2	0.4	0.577	0.0081	0.0049		
	−1.8	−7.1	−2.3	0.592	0.0035	0.0037		
95-I-24	−1.0	−4.6	−0.2	0.602	0.0077	0.0139	0.589 ± 0.007	38.8 ± 2.1
	−1.0	−4.5	0.6	0.586	0.0081	0.0118		
	−1.0	−4.6	1.0	0.578	0.0075	0.0052		
Bouse Formation (4–9 Ma)								
96BS1	0.6	−5.0	−2.6	0.644	0.0077	0.0147	0.648 ± 0.003	24.7 ± 1.1
	0.5	−4.9	−2.8	0.651	0.0078	0.0148		
95BS8	0.0	−6.6	−6.4	0.695	0.0074	0.0133	0.660 ± 0.018	22.1 ± 3.8
	0.1	−6.5	−3.7	0.636	0.0087	0.0133		
	0.1	−6.6	−4.3	0.648	0.0074	0.0050		
95BS10	0.5	−5.4	−1.4	0.610	0.0076	0.0144	0.623 ± 0.013	30.5 ± 3.0
	0.5	−5.5	−2.6	0.635	0.0074	0.0054		
95BS17	1.6	−9.0	−5.9	0.629	0.0074	0.0127	0.622 ± 0.007	30.8 ± 1.8
	1.7	−9.2	−5.3	0.614	0.0071	0.0108		
96BS24	0.6	−5.1	−1.6	*0.621*	*0.0077*	*0.0105*	0.629 ± 0.008	29.0 ± 2.0
	−2.0	−9.0	−6.2	*0.636*	*0.0079*	0.0043		
96BS25	−5.5	−9.7	−6.3	0.623	0.0081	0.0123	0.623 ± 0.001	30.4 ± 0.9
	−5.5	−9.5	−6.0	0.621	0.0077	0.0045		
	−5.6	−9.6	−6.3	0.625	0.0076	0.0045		
Hualapai Limestone (~6 Ma)								
96HU2	1.0	−11.6	−7.2	0.600	0.0089	0.0105	0.616 ± 0.016	32.1 ± 4.0
	1.0	−11.5	−8.5	0.632	0.0090	0.0043		
96HU5	1.6	−11.4	−8.3	0.629	0.0076	0.0104	0.627 ± 0.002	29.6 ± 1.1
	1.6	−11.5	−8.1	0.624	0.0093	0.0044		
Bidahochi Formation, Upper (Younger Than 6 Ma)								
98B11a	−5.4	−11.4	−8.9	*0.643*	*0.0072*	0.0100	0.647 ± 0.003	24.9 ± 1.0
	−5.4	−11.3	−9.3	*0.653*	*0.0096*	0.0099		
	−5.4	−11.4	−9.0	*0.645*	*0.0076*	0.0099		
98B11b	−5.1	−11.6	−9.8	0.658	0.0107	0.0099	0.652 ± 0.008	23.7 ± 2.0
	−5.1	−11.5	−9.8	0.660	0.0077	0.0099		
	−5.1	−11.5	−9.9	0.663	0.0086	0.0099		
	−5.1	−11.5	−8.4	0.629	0.0085	0.0099		
Bidahochi Formation, Lower (~16 Ma)								
99B21	−2.4	−8.5	−7.0	0.665	0.0132	0.0105	0.660 ± 0.013	22.1 ± 2.9
	−2.4	−8.6	−6.5	0.652	0.0100	0.0043		
	−2.4	−8.8	−5.0	0.615	0.0067	0.0105		
	−2.4	−8.6	−8.0	0.685	0.0083	0.0043		
	−2.4	−8.7	−7.9	0.681	0.0097	0.0086		
99B22	−1.9	−4.4	−0.4	0.610	0.0080	0.0114	0.653 ± 0.022	23.6 ± 5.0
	−1.9	−4.4	−3.0	0.668	0.0074	0.0051		
	−1.8	−4.5	−3.7	0.680	0.0092	0.0102		
98B4	−1.4	−6.0	−3.8	0.650	0.0075	0.0096		24.2 ± 1.9
Rainbow Gardens Member, Horse Spring Formation (18–26 Ma)								
07KH12	−2.9	−11.9	−7.9	0.610	0.0071	0.0122	0.610 ± 0.0002	33.6 ± 0.1
	−3.0	−11.8	−7.8	0.610	0.0069	0.0045		
07KH14	−1.8	−10.2	−6.0	0.606	0.0068	0.0108	0.620 ± 0.015	31.0 ± 3.8
	−2.0	−10.1	−7.3	0.635	0.0091	0.0043		
Westwater Formation (45–55 Ma)								
07KH01	−4.5	−5.3	1.2	0.558	0.0075	0.0117		47.1 ± 3.5
Rim Gravels (45–55 Ma)								
DB4-1	−6.5	−14.5	−12.5	0.653	0.0102	0.0108		23.6 ± 2.4
DB4-2	−6.6	−14.4	−9.8	0.597	0.0067	0.0076		36.8 ± 2.0
DB4-3	−9.2	−14.3	−3.7	0.477	0.0077	0.0165	0.482 ± 0.0049	70.4 ± 3.0
	−9.1	−14.3	−4.3	0.487	0.0080	0.0165		

change, previous studies have calculated paleoelevation differences from comparisons of MAT estimates from materials deposited at the same latitude and time [e.g., *Axelrod*, 1966]. Here we use an analogous approach to infer paleoelevation based on temperature estimates from clumped isotope thermometry in the Colorado Plateau region. Such an approach is potentially advantageous because while changes in flora reflect changes in climatic variables such as aridity as well as changes in temperature, clumped isotope thermometry is sensitive to temperature alone.

3.3. Sampling Strategy for Application to the Colorado Plateau

[19] Samples were collected with three goals in mind: (1) to evaluate what forms of terrestrial carbonate preserve a high-fidelity record of primary surface water temperature and $\delta^{18}O$; (2) to characterize spatial and temporal changes in temperature in the Colorado Plateau region; and (3) to develop a framework for reconstructing paleoelevation from ancient temperatures based on the correlation between temperature and elevation recorded by modern samples. While our primary target was the Bidahochi Formation (section 2.3), complementary ancient and modern samples provide critical context for interpretation of the Bidahochi Formation results.

[20] The 21 ancient samples we examined consist of diverse materials including gastropods, the bivalve *anomia*, oysters, barnacles, soil, marl, tufa, and limestone from Cretaceous to Pliocene deposits from and adjacent to the plateau (Table 1 and Figure 1). Clumped isotope data for two of these samples, 95I23 and 95I24, were previously reported in an analytical methods paper by *Huntington et al.* [2009], although their geologic significance was not discussed. In some cases it was possible to sample several different kinds of carbonate from the same paleoenvironment in order to evaluate variability in the temperature signal (e.g., Horse Spring Formation samples, Table 1). We selected samples for which independent observations (e.g., petrographic analysis, geologic evidence, or Sr/Ca values [cf. *Spencer and Patchett*, 1997]) suggested the carbonate was primary. These include Bidahochi Formation, Bouse Formation, and Hualapai Formation samples from the collection of J. Patchett for which previous geochemical analyses were reported by *Gross et al.* [2001] and *Spencer and Patchett* [1997]. For the remaining samples, primary material was selected on the basis of petrographic analysis. We sampled multiple stratigraphic levels within the same unit to investigate temporal shifts in temperature, and also sampled units of the same depositional age found at different modern elevations. Based on clumped isotope analysis of 50 aliquots from the 21 ancient samples (Table 1), we determined what materials likely record depositional conditions. We then collected similar materials from modern environments in 9 localities to establish the relationship between temperature recorded by clumped isotope thermometry, modern water and air temperature, and modern elevation (Table 2 and Figure 1).

4. Analytical Methods

[21] Carbonate powders were collected from fresh interior surfaces of the samples using a microdrill or razor and then ground gently using a mortar and pestle. The isotopic composition of CO_2 produced by acid digestion of the resulting powders was measured by dual-inlet isotope ratio gas source mass spectrometry at the California Institute of Technology. CO_2 was produced by anhydrous phosphoric acid digestion of ~8 mg of carbonate powder from each sample at 25°C for 12–24 h using a McCrea-type reaction vessel [*McCrea*, 1950; *Swart et al.*, 1991]. Product CO_2 was isolated and purified by conventional cryogenic procedures using the glass vacuum apparatus described by *Ghosh et al.* [2006a]. Even ppb level contaminants can lead to significant apparent changes in Δ_{47}. Thus additional measures were taken to purify samples, namely, sample CO_2 was entrained in He carrier gas flowing at a rate of 3 ml/min and passed through an Agilent Tech 6890N gas chromatograph (GC) column (Supel-Q-PLOT column with 530 μm internal diameter, 30 m long) held at −10°C, and collected for 40 min.

Notes to Table 1:

[a]See auxiliary material for complete results. Imperial, Bouse and Hualapai samples were collected by *Spencer and Patchett* [1997], who reported Sr isotope results for samples 95-I-23, 96BS1, 95BS17, 96BS25, 96HU2, and 96HU5. *Huntington et al.* [2009] reported clumped isotope thermometry data for 95-I-23 and 95I24 but did not comment on their significance. Results for Bouse Formation samples 95BS1 and 95BS12 not shown in summary table because all replicates (n = 5) exhibited evidence of contamination (i.e., high Δ_{48}). Sr isotopic results for Bidahochi samples were reported previously by *Gross et al.* [2001]. Unit age constraints come from the following sources: Imperial Formation, *Ingle* [1973, 1974] and *Winterer* [1975]; Bouse Formation, *Johnson et al.* [1983], *Buising and Baratan* [1993], and *Winker and Kidwell* [1986]; Hualapai Limestone, *Spencer et al.* [2001] and *Wallace et al.* [2005]; Bidahochi Formation, *Dallegge* [1999] and *Gross et al.* [2001, and references therein]; Rainbow Gardens, *Beard* [1996] and *Lamb et al.* [2005]; Westwater Formation, *Young* [1999]; Rim Gravels, [*Holm*, 2001].

[b]Sample information is as follows: 95-I-23, Fish Creek area (32 58.57N, 116 9.26W, deposited at sea level, oyster; 95-I-24, Fish Creek area (32 58.57N, 116 9.26W), deposited at sea level, *anomia sp.*; 96BS1, Cibola area, Arizona (33 15.41N, 114 38.47W), elevation 125 m, micrite; 95BS8, Cibola area, Arizona (33 15.41N, 114 38.47W), elevation 110 m, micrite; 95BS10, Cibola area, Arizona (33 15.41N, 114 38.47W), elevation 100 m, calc siltstone; 95BS17, Milpitas Wash, California (33 15.54N, 114 43.73W), elevation 88 m, barnacle; 96BS24, Silver Creek, Arizona (35 5.23N, 114 28.13W), elevation 535 m, marl; 96BS25, Silver Creek, Arizona (35 5.23N, 114 28.13W), elevation 536 m, marl; 96HU2, SW of Temple Bar (35 58.48N, 114 24.84W), elevation 646 m, limestone; 96HU5, SW of Temple Bar (35 58.49N, 114 20.73W), elevation 640 m, limestone; 98B11a, Eastern Lake margin (35 36.80N, 109 44.13W), elevation 1870 m, lake edge tufa; 98B11b, Eastern Lake margin (35 36.80N, 109 44.13W), elevation 1870 m, lake edge tufa; 99B21, Yellow Butte, Arizona (35 25.09N, 110 21.89W), elevation 1898 m, marl; 99B22, Yellow Butte, Arizona (35 25.09N, 110 21.89W), elevation 1898 m, marl; 98B4, Echo Spring Mt., Arizona (35 18.85N, 110 12.68W), elevation 1806 m, marl; 07KH12, Tassai Wash, Nevada (36 15.152N, 113 57.199W), elevation 625 m, soil rip up; 07KH14, Tassai Wash (36 15.152N, 113 57.199W), elevation 628 m, micrite; 07KH01, Milkweed Canyon, Arizona (35 38.725N, 113 41.708W), elevation 1269 m, limestone; DB4-1, Duff Brown Tank (35 36.48N, 112 36.27W), elevation 1780 m, sparry calcite cement; DB4-2, Duff Brown Tank (35 36.48N, 112 36.27W), elevation 1780 m, matrix calcite; DB4-3, Duff Brown Tank (35 36.48N, 112 36.27W), elevation 1780 m, calcified gastropod shell.

Table 2. Summary of Clumped Isotope Thermometry and Stable Isotopic Results for Modern Lake Carbonates[a]

Sample[b]	$\delta^{13}C_{PDB}$ (‰)	$\delta^{18}O_{PDB}$ (‰)	$\delta^{18}O_{SMOW}$ (‰)	Δ_{47} (‰)	Analytical 1 SE Δ_{47} (‰)	1 SE Δ_{47} (‰)	Summary	
							Average Δ_{47} (‰)	Temperature ±1 SE (°C)
ME	−8.7	−9.2	−7.3	0.655	0.0090	0.0105	0.657 ± 0.002	22.7 ± 0.7
	−9.3	−9.0	−7.1	0.655	0.0073	0.0084		
	−8.7	−11.1	−9.4	0.661	0.0033	0.0037		
MO	7.1	−1.8	−1.6	0.695	0.0069	0.0193	0.682 ± 0.006	17.3 ± 1.5
	7.1	−2.2	−1.3	0.679	0.0075	0.0189		
	7.1	−3.9	−2.7	0.674	0.0036	0.0094		
CR	−1.9	−16.9	−17.5	0.714	0.0078	0.0081	0.681 ± 0.017	17.7 ± 3.5
	−0.4	−14.4	−12.7	0.661	0.0078	0.0113		
	−1.1	−15.6	−14.2	0.668	0.0080	0.0099		
BE	−5.1	−16.2	−16.0	0.727	0.0078	0.0130	0.702 ± 0.016	13.4 ± 3.2
	−3.3	−12.9	−12.0	0.697	0.0070	0.0097		
	−5.0	−14.6	−13.5	0.658	0.0069	0.0090		
	−4.0	−14.6	−13.0	0.724	0.0072	0.0086		
EM	−1.1	−13.6	−15.0	0.732	0.0073	0.0091	0.721 ± 0.012	9.6 ± 2.4
	0.8	−10.2	−9.8	0.690	0.0064	0.0088		
	−0.1	−11.9	−12.6	0.716	0.0094	0.0086		
	−0.2	−11.5	−13.6	0.748	0.0077	0.0073		
SG	−3.0	−14.6	−16.3	0.739	0.0093	0.0105	0.718 ± 0.023	10.2 ± 4.4
	−3.3	−15.0	−13.8	0.673	0.0075	0.0085		
	−2.9	−14.6	−16.4	0.742	0.0072	0.0082		

[a]Core top sediment samples obtained from L. Anderson (USGS, Denver). Results for Deep Springs (DS, 1498 m), Owens Lake (OW, 1147 m), and Walker Lake (WA, 1190 m) exhibited evidence of contamination (i.e., high Δ_{48}) and are not included in summary table.

[b]Sample information is as follows: ME, Lake Mead, Nevada (36.30214N, 114.41845W), 372 m, lake edge precipitate; MO, Mono Lake, California (37.94406N, 119.02741W), 1899 m, tufa; CR, Lake Crowley, California (37.58176N, 118.7392W), 2058 m, lake edge precipitate; BE, Blue (Eagle) Lake, Colorado (39.753265N, 106.764134W), 2552 m, core top sediment; EM, Emerald Lake, Utah (39.074272N, 111.497257W), 3093 m, core top sediment; SG, south Grizzly Creek Lake, Colorado (39.690184N, 107.319730W), 3242 m, core top sediment.

After evacuation of the He carrier gas, conventional cryogenic procedures were repeated twice to purify the sample before condensation into an evacuated glass vessel for transfer to the mass spectrometer.

[22] Isotopic analysis of CO_2 was performed on a Finnigan MAT 253 mass spectrometer configured to measure masses 44–49 after the methods of *Eiler and Schauble* [2004]. Each analysis required 3 to 4 h of mass spectrometer time to achieve precisions of 10^{-6} (thousandths of per mil) in Δ_{47}, and multiple replicate analyses of each sample were performed to reduce temperature uncertainties to as good as ±1–2°C (1 SE) [e.g., *Huntington et al.*, 2009]. As a consequence, sample throughput was limited, requiring 1 to 2 days of mass spectrometer analysis for a single temperature determination (compared to the ~80–100 conventional stable isotopic measurements of $\delta^{18}O$ and $\delta^{13}C$ that can be performed per day using an automated device [e.g., *de Groot*, 2009]). Values for $\delta^{13}C$ reported versus VPDB and $\delta^{18}O$ reported versus VSMOW were calculated using the program Isodat 2.0 and standardized by comparison with CO_2 evolved from phosphoric acid digestion of the NBS-19 carbonate standard distributed by the International Atomic Energy Agency. Measurements of Δ_{47} were made using the methods of *Eiler and Schauble* [2004] and changes in sample preparation of *Affek and Eiler* [2006]. Values of Δ_{47} were calculated based on raw measurements of R^{45}, R^{46}, and R^{47}, where R^i is the abundance of mass i relative to the abundance of mass 44, using the methods of *Affek and Eiler* [2006] and *Wang et al.* [2004]. Values of Δ_{47} were normalized using measurements of CO_2 heated to achieve the stochastic distribution of isotopologues and errors were propagated as detailed by *Huntington et al.* [2009]. Measurements of Δ_{48} for the samples were used to screen for contaminants such as sulfur, hydrocarbons, and organics, through comparison of Δ_{48} for clean heated CO_2 [*Eiler and Schauble*, 2004; *Guo and Eiler*, 2007; *Huntington et al.*, 2009]. Stable isotopic results ($\delta^{13}C$, $\delta^{18}O$, and Δ_{47}) for ancient samples are summarized in Table 1 and Figure 2. Results for modern samples are summarized in Table 2 and Figures 2 and 3. Isotopic results are presented in full in the auxiliary material, including measurements of Δ_{48}.[1]

5. Carbonate Growth Temperature and O Isotopic Results

5.1. Cretaceous to Pliocene Carbonates

[23] Carbonate clumped isotope temperatures and $\delta^{18}O$ values for various kinds of carbonates from Cretaceous to Pliocene deposits from paleoenvironments presently exposed at elevations from sea level to 1900 m are reported in Table 1 and Figure 2. The abundances of ^{13}C-^{18}O bonds in these materials correspond to temperatures between 22.1 and 70.4°C, and the average precision in temperature estimates for independent replicates of the same sample is ±2.3°C (1 SE). Bulk isotopic compositions of these carbonates range from −9.2 to +1.7‰ for $\delta^{13}C_{PDB}$ and −14.5 to −4.4‰ for $\delta^{18}O_{PDB}$, with typical uncertainties of ±0.1‰ (1 SE). Calculated values of $\delta^{18}O_{smow}$ for water in equilibrium with carbonate range from −12.5 to +1.2‰.

[1]Auxiliary materials are available at ftp://ftp.agu.org/apend/tc/2009TC002449.

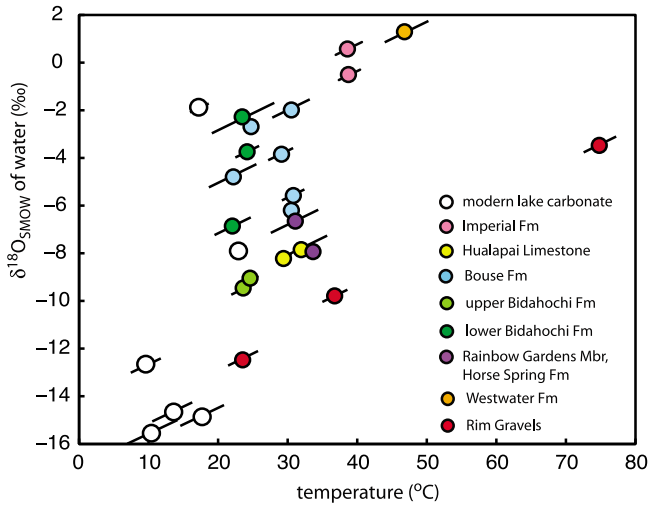

Figure 2. Temperature estimates from clumped isotope thermometry versus $\delta^{18}O$ of water in equilibrium with the carbonate for modern and ancient samples listed in Tables 1 and 2. The $\delta^{18}O$ of water was calculated from measured $\delta^{18}O$ of carbonate and temperature from Δ_{47}, using the carbonate-water fractionation factor of *Kim and O'Neil* [1997].

[24] Whereas samples at the lower end of the observed temperature range could represent crystallization at or near Earth surface conditions and thus constrain paleoelevation and climate, samples yielding temperatures in excess of ~33°C likely record carbonate recrystallization and replacement during diagenesis and/or burial metamorphism ("resetting"). Some of the temperatures in excess of plausible near-surface conditions occur in carbonates that also have anomalously high $\delta^{18}O$ values (Figure 2). The most easily interpreted of these reset materials are gastropod fossils from the Rim Gravels in which original aragonite is completely replaced by calcite (70.4 ± 3.0°C). The Rim Gravel samples likely experienced reheating due to nearby emplacement of a Miocene basalt flow [*Young*, 1999]. More cryptic resetting is observed in a suite of Pliocene molluscs from tidal flat facies of the Imperial Formation (~39°C), and limestone from the Westwater Formation (47.1 ± 3.5°C). Although the $\delta^{18}O$ values of the Imperial Formation samples do not indicate resetting a priori, temperatures 6–8°C in excess of the reasonable range for mollusk shell precipitation and reproduction indicate that resetting has taken place. The Westwater Formation sample's stratigraphic location, elevated temperature, and elevated $\delta^{18}O$ value are consistent with resetting during burial.

[25] Most samples that we interpret to be unreset (i.e., because they yield temperatures within the plausible Earth surface range and show no evidence of alteration) are fine-grained micrites. Other unreset samples included soil carbonates, barnacles, and tufa. Although we have no reason to suspect on the basis of textural or other evidence that these samples were reset, it is nevertheless possible that resetting took place, shifting temperatures by a few degrees but not to values outside of the range of Earth surface conditions. We are not aware of a way to disprove this possibility; however, we note that a correlation of temperatures for samples of a given age range with altitude would not be expected to result from diagenetic resetting.

[26] Carbonates from the mid-Miocene to Pliocene Bidahochi, Bouse, and Hualapai formations all record temperatures within the range plausible for carbonate growth at the Earth's surface during spring to summer and oxygen isotopic compositions consistent with them having grown from waters similar in $\delta^{18}O$ to modern surface waters in the Colorado River drainage (Figure 2) [*Guay et al.*, 2006]. Bidahochi Formation tufas and marls from modern elevations of 1806 to 1989 m in the upper basin of the Colorado River record depositional temperatures over the narrow range of 22.1–24.9°C, with no systematic difference in temperature in samples from 16 Ma and 6 Ma deposits. Assuming the scatter in ages is Gaussian, the weighted mean temperature is 23.5 ± 1.0°C. The range of depositional temperatures recorded by lacustrine carbonates from the Bouse and Hualapai formations cropping out at modern elevations of 88 to 646 m in the lower basin of the Colorado River is much greater, 22.1–32.1°C. The large range in temperatures results primarily from the two lowest recorded temperatures, 22.1 ± 3.8°C and 24.7 ± 1.1°C. These samples were obtained from lower Bouse carbonates from the southernmost section, which is currently only 100 m above sea level. A third sample from the same location, located at the bottom of the section, yielded a warmer temperature of 30.5°C. This temperature, plus the remaining five analyses from the lower basin all overlap within one standard error, ranging from 29.0 to 32.1°C.

5.2. Modern Carbonates

[27] To enable direct comparison of modern and ancient lake carbonates, we collected and analyzed materials similar to the ancient samples from modern lakes from 350 to 3300 m elevation in the southwestern United States (Figure 1). Growth temperatures and bulk isotopic compositions of these materials, which include core top sediments and tufa, are summarized in Table 2 and Figures 2 and 3. Of 27 analyses of diverse carbonates collected from 9 modern localities, analysis of materials from 3 of the 9 samples (7 of 27 analyses) showed evidence of contamination from hydrocarbons or organics (i.e., high Δ_{48}), and had to be rejected. A variety of purification methods in addition to the standard cryogenic and GC techniques were attempted to remove the contaminants (e.g., hydrogen peroxide), but none was completely successful. Temperatures for the uncontaminated samples ranged from 9.6 to 22.7°C, with average precision of ±2.6°C. Higher variability was observed among analyses of different aliquots of sediment collected from the top 0.5 to 1.5 cm of lake cores, reflecting inhomogeneity of the samples. Isotopic values for the carbonates range from −9.3 to 7.1‰ for $\delta^{13}C_{PDB}$ and −16.9 to −1.8‰ for $\delta^{18}O_{PDB}$. Values of $\delta^{18}O_{smow}$ for water in equilibrium with carbonate span a large range from −17.5 to −1.3‰, consistent with the large range of values observed for modern surface waters in the Colorado River drainage [e.g., *Guay et al.*, 2006]. The correlation between temperature measured from clumped

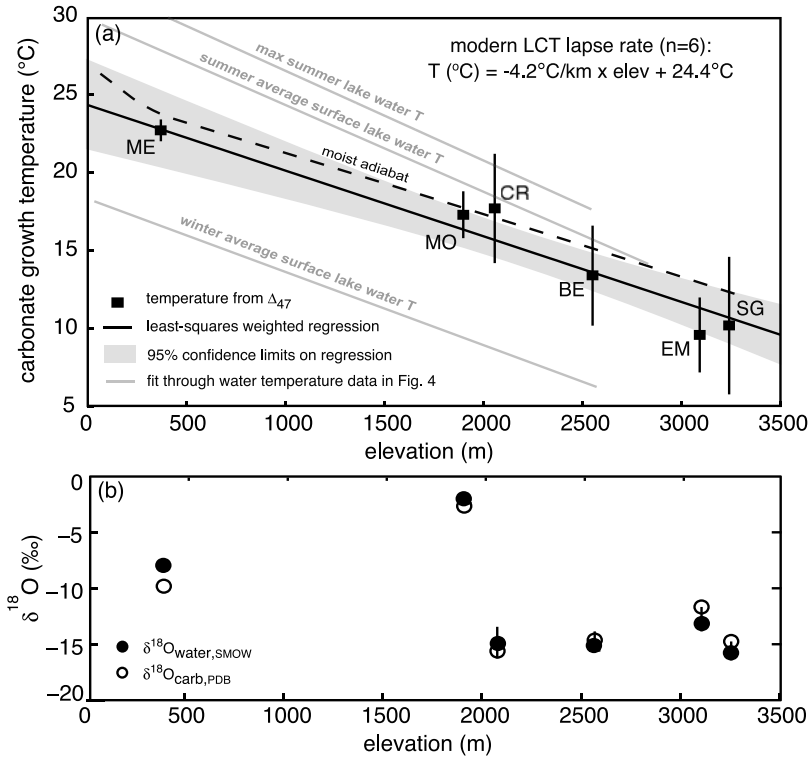

Figure 3. (a) Comparison of midlatitude semiarid lake surface water temperatures, modeled moist adiabat, and temperature estimates from modern carbonate sediments precipitated in lake waters as a function of elevation. Black squares represent clumped isotope thermometry results for modern lake carbonates listed in Table 2, with 1σ errors. Samples ME, BE, EM, and SG were collected within the modern Colorado River drainage. Solid line indicates best fit error-weighted linear least squares regression through the temperature-elevation data [*York*, 1968]. Best fit water surface temperature lines (gray) are given by regressions through the data shown in Figure 4. Dashed black line indicates modeled "moist adiabat" lapse rate for 85% relative humidity [*Schneider*, 2007] for reference. (b) Open circles indicate δ^{18}O of carbonate for the samples shown in Figure 3a versus elevation. Black circles indicate δ^{18}O of the water in equilibrium with the carbonate versus sample elevation.

isotopes and modern lake elevation is excellent (r = 0.97), with temperature values typical of spring and early summer surface waters (Figure 3).

5.3. Trends in O Isotopic Values Versus Elevation and Distance Inland

[28] The temperature differences observed for the modern and ancient carbonates correspond to differences in the δ^{18}O of water from which they grew (Table 1 and Figure 2). The δ^{18}O values of water in equilibrium with the modern carbonates (n = 6) are correlated with elevation (r = 0.55) and with distance from the coast (r = 0.61) (Figure 3b, 4). The δ^{18}O values of the waters from which the unreset ancient samples (n = 13) grew also are weakly correlated with modern elevation (r = 0.34), broadly consistent with the notion that the ancient samples record depositional temperatures and have not been reset. The modern and ancient data are broadly consistent with one another when plotted versus distance inland or versus elevation (Figure 4). When taken together, their δ^{18}O values of water in equilibrium with the carbonates exhibit an isotopic lapse rate of 3‰ per 1 km of elevation, with a correlation coefficient r of 0.70 (Figure 4b). The δ^{18}O of water values for the ancient samples are more highly correlated with inferred distance from the coast at the time of deposition (r = 0.55, Figure 4a) than with modern elevation, with the southernmost Bouse (Cibola area) samples plotting slightly below oceanic δ^{18}O values. The combined modern and ancient carbonate O isotopic data reveal a decreasing trend of 0.9‰ per 100 km of distance inland from the coast at the time of deposition (r = 0.77, Figure 4a), consistent with the notion that data for mid-Miocene to modern carbonates generally follow the same trend.

6. Discussion

6.1. Depositional Temperatures of Terrestrial Carbonates: What Worked and What Did Not

[29] Clumped isotope thermometry of Tertiary carbonates from and adjacent to the Colorado Plateau reveals that many terrestrial carbonates record reasonable depositional temperatures and δ^{18}O values, provided they were never deeply buried. Although we do not know of a way to disprove the possibility that subtle resetting (i.e., by a few degrees) has

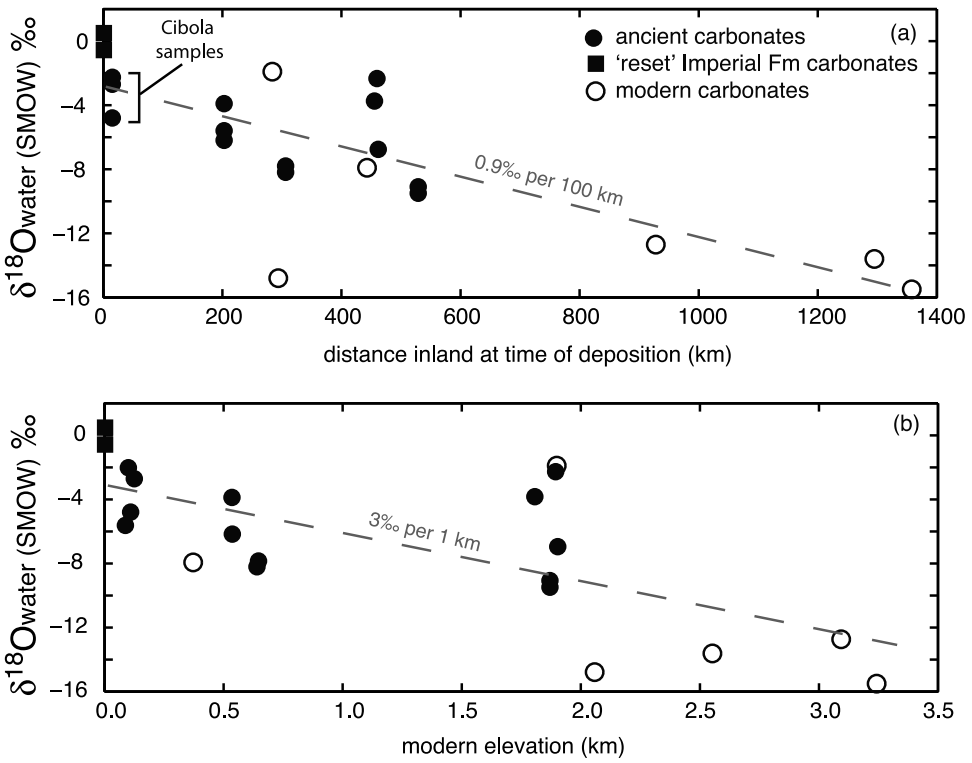

Figure 4. O isotope results for modern and ancient carbonates versus elevation and inland distance. (a) The δ^{18}O of the water in equilibrium with the carbonate versus distance inland at the time of deposition. Closest linear distance inland is plotted for modern samples. For the ancient carbonates, the Cibola samples were taken to be 15 km from the coast at the time of deposition. Distance inland for the other ancient carbonates was measured relative to the Cibola samples. Marine water plots at 0‰. (b) The δ^{18}O of the water in equilibrium with the carbonate versus modern elevation above sea level of the deposit. Modern carbonate data are also plotted in Figure 3b. In Figures 4a and 4b, the dashed lines indicate the simple best fit linear regression through the modern and ancient data. The Imperial Formation samples are plotted for reference.

taken place in the samples we have interpreted as primary, measured temperature and elevation are correlated, suggesting that depositional temperatures have been recorded. In most cases, independent information (e.g., anomalously high δ^{18}O, geologic evidence of burial substantially greater than 100 m, nearby volcanism, or nonprimary mineralogy) also indicated that samples with measured temperatures in excess of plausible surface temperatures must have been reset. Although fossils are tempting targets for carbonate clumped isotope thermometry because of their relation to modern taxa with known habits and because fossil assemblages can provide tight age constraints, our results are consistent with the findings of *Came et al.* [2007] suggesting that they are highly vulnerable to resetting. In contrast, fine-grained micrites and tufa consistently yield temperatures within the plausible Earth surface range.

6.2. Temperature Versus Elevation Trends

6.2.1. Modern Samples

[30] Carbonate growth temperatures for the modern samples correlate strongly with elevation (r = 0.97), defining a lake water carbonate temperature (LCT) lapse rate of 4.2°C/km with a zero elevation intercept of 24.4°C (Figure 3a). In contrast, we observe a significantly weaker correlation between δ^{18}O measured for modern lake carbonates and elevation (r = 0.55; Figures 3b and 4). The weaker correlation between δ^{18}O and elevation may reflect variations in evaporative enrichment or hydrology of the sampled lakes, which do not vary systematically with altitude, but nonetheless impact the δ^{18}O of water.

[31] The ancient LCT measurements are comparable to modern lake water temperatures in the Colorado Plateau region. A compilation of modern temperature observations for surface waters in Arizona yields lacustrine surface water temperature (LST) lapse rates of 4.8 and 5.8°C/km for winter and summer months, respectively, although considerable scatter is observed (Figure 5a). The LCT curve falls between the winter and summer curves, which have zero elevation intercepts at roughly 18 and 30°C, respectively (Figure 3a). The LCT curve never exceeds the maximum summer temperatures observed for a subset of well-monitored lakes and reservoirs at elevations from sea level to 2550 m in the plateau and environs (Figures 3a and 6b).

[32] The observed LCT lapse rate is indistinguishable from the moist adiabat for the atmosphere (85% relative

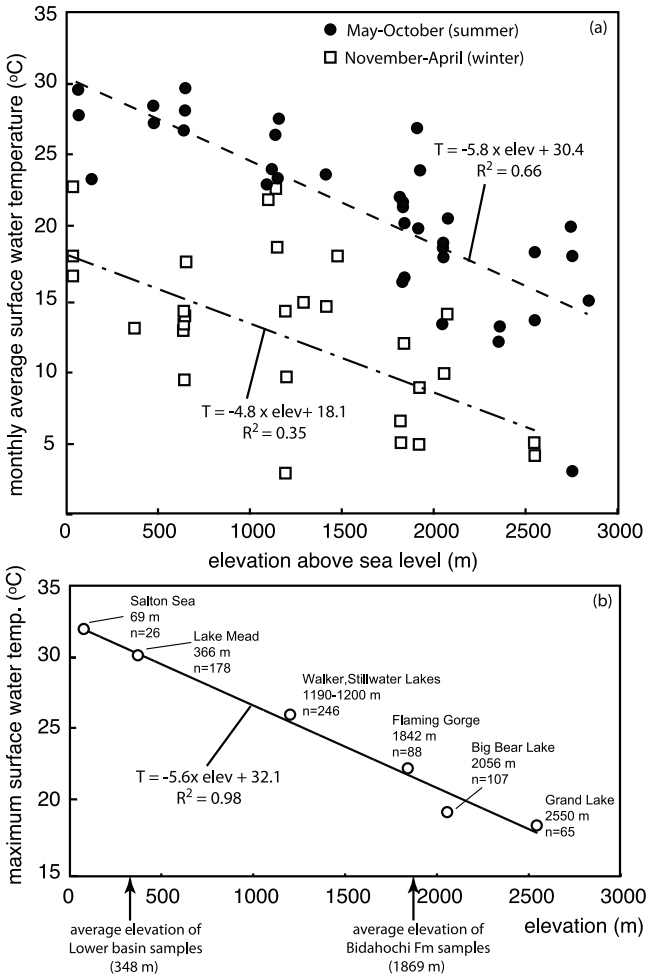

Figure 5. Lake surface water temperature (LST) measurements made between 1979 and 2007 for Colorado Plateau area surface waters compiled from U.S. Geological Survey water resources data (http://waterdata.usgs.gov). (a) Surface water temperature measurements for lakes, ponds, and reservoirs in Arizona versus elevation above sea level, binned according to season in which the measurement was made (summer months are black circles; winter months are open squares). Dashed and dash-dotted lines indicate LST lapse rates based on simple linear regression through data for summer and winter months, respectively. (b) Maximum surface water temperature observed between 1979 and 2007 for well-monitored water bodies in the Colorado Plateau region, where n indicates the number of temperature observations for each water body.

humidity, Figure 3a), but less than the LST lapse rates for winter and summer months and the lapse rate defined by lake surface maximum temperatures (5.6°C/km; Figure 5b). Lapse rates based on lake water temperatures in turn are less than the MAT [*Meyer*, 1992] and representative monthly air temperature lapse rates for the region of 6.8 to 8.1°C/km (Figure 6). The slopes of the LCT and LST trends are not as steep as air temperature lapse rates, presumably due to the greater direct influence of the atmosphere on the temperatures of surface waters in stratified lakes.

[33] The position of the LCT trend between the more steeply sloping LST winter and summer curves is most likely due to the timing, depth, and temperature of calcium carbonate saturation in lakes. During cold months lake water temperatures vary little with depth (Figure 7a). As surface waters warm in spring and summer, a stable thermocline develops, suppressing mixing between warm, buoyant near-surface waters (epilimnion) and cold, dense bottom waters (Figure 7a). In the spring and summer, evaporation is enhanced and carbonate solubility is depressed in the epilimnion, causing growth of microcrystalline carbonate (whiting events) to occur [e.g., *Duston et al.*, 1986; *Effler et al.*, 1987]. Warm water, abundant sunlight, and nutrients also promote algae growth in the upper few meters, which enhances supersaturation by increasing pH and provides nucleation sites – both of which promote carbonate precipitation [*Stunm and Morgan*, 1981]. Thus carbonate growth temperatures should reflect spring to summer near-surface temperatures, with little sensitivity to lake depth because carbonate production primarily occurs within the epilimnion. A comparison of our modern Lake Mead carbonate growth temperatures and detailed water temperature records supports this hypothesis (Figure 7b) and provides empirical evidence that growth temperatures of lacustrine carbonates measured using carbonate clumped isotope thermometry reflect lake water temperatures that are strongly correlated with elevation. However, it is important to note that as a first step toward characterizing the modern LCT lapse rate we analyzed only one sample from each locality, and as a consequence we do not have enough data to identify probable Holocene variability in lacustrine carbonate temperatures.

6.2.2. Ancient Samples

[34] Our primary goal was to determine paleoelevation of the ~16–6 Ma Bidahochi Formation to constrain the uplift history of the southern Colorado Plateau. The recorded Bidahochi Formation temperatures near ~24°C do not vary within the error of the measurements. The results imply that elevation changes of more than a few hundred meters, or climate variation of more than 3°C did not occur during deposition from 16 to 6 Ma, presuming that larger changes in both elevation and climate did not conspire to keep the temperatures relatively constant.

[35] If the modern carbonate temperature versus elevation measurements were to apply to Middle and late Miocene time, the temperature data would imply that the Bidahochi Formation was deposited at about 400 m elevation, near the modern elevation of Lake Mead (Figure 3a), indicating 1400 m of uplift since 6 Ma. This estimate does not, however, account for climate change, in particular the likelihood that the Miocene climate was much warmer than the interglacial climates typical of the Quaternary. An important role for climate is suggested by the lower basin samples. Although the scatter in lower basin temperature estimates is large (10°C), their average temperature is 4–5°C warmer than the modern LCT curve (Figure 3a).

[36] As noted in section 5.1, the scatter in lower basin temperatures is primarily the result of the two lowest elevation samples. The remaining six estimates have a weighted

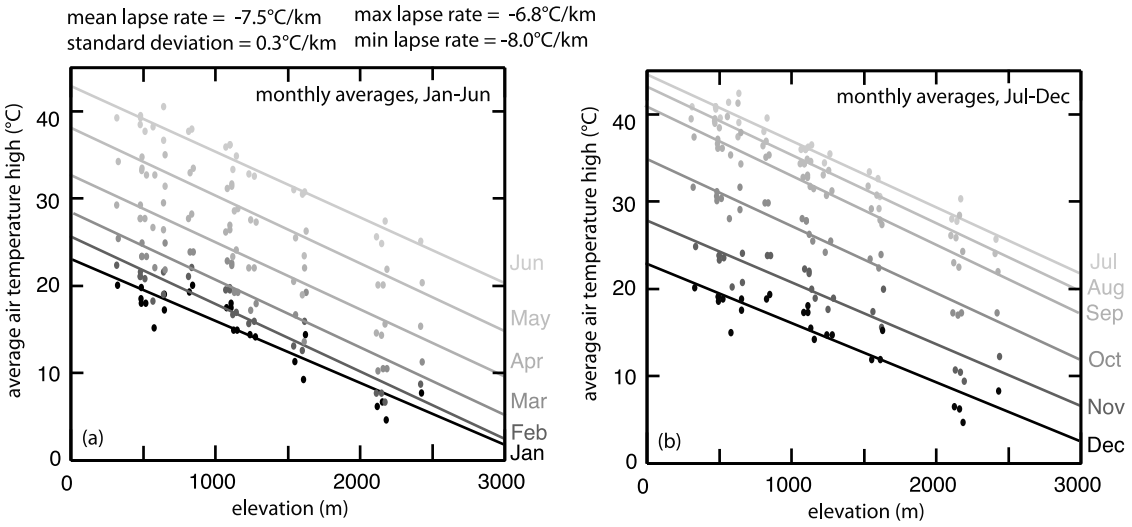

Figure 6. Air temperature lapse rates based on average of monthly air temperature highs recorded at 24 Arizona weather stations from 341 to 2441 m elevation above sea level between 1971 and 2000, compiled from the Desert Research Institute's Western Regional Climate Center data (http://www.wrcc.dri.edu). (a) Monthly average temperatures for January–June, with simple best fit linear regression. (b) Monthly average temperatures for July–December, with simple best fit linear regression.

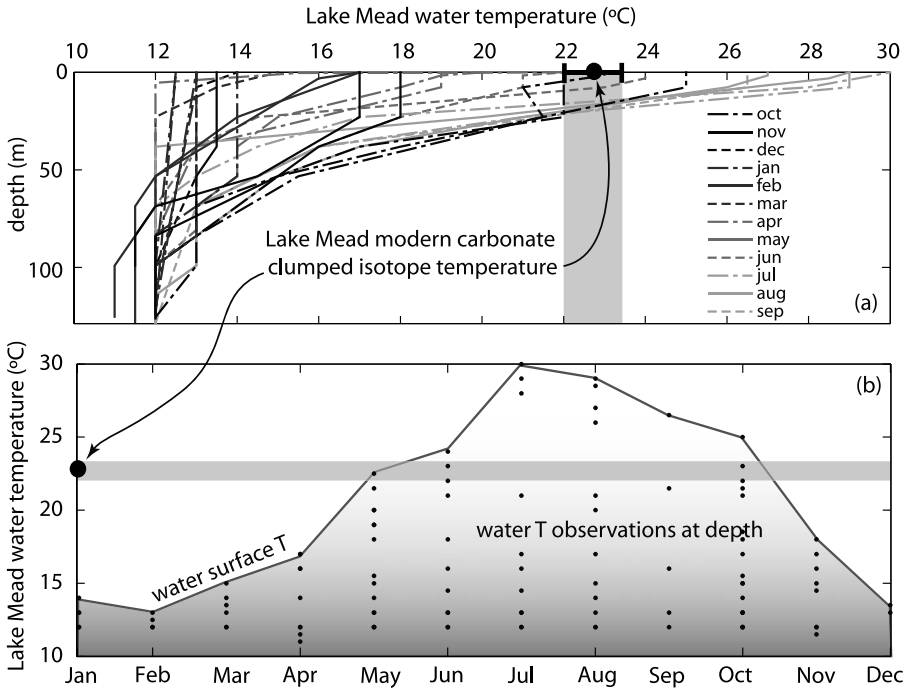

Figure 7. Lake Mead water temperature data compiled from U.S. Geological Survey water resources data (http://waterdata.usgs.gov). (a) Water temperature versus depth profiles indicated by month during which observations were made. (b) Water temperature versus month during which observations were made. The measured clumped isotope temperature of modern carbonate precipitated from Lake Mead (ME, Table 2) indicated is consistent with carbonate precipitation during spring/summer months (May–October), from near-surface lake waters.

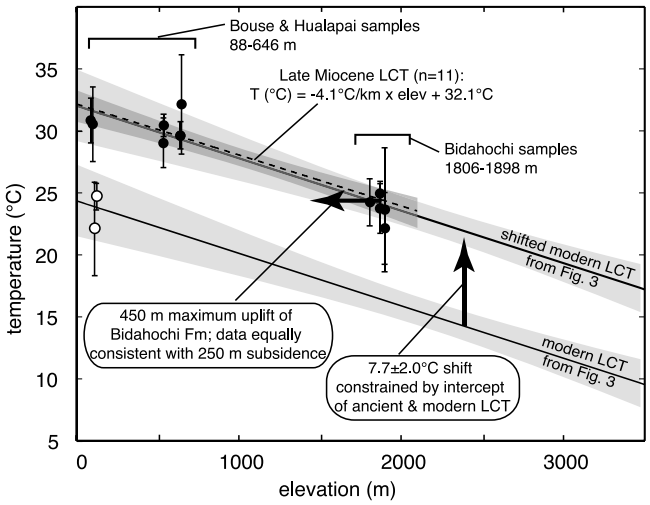

Figure 8. Carbonate clumped isotope thermometry temperature estimates versus modern elevation for samples collected in the Colorado River basin. Data points marked by open circles are interpreted to reflect cooling of lake surface temperatures by a marine climate; horizontal arrow indicates magnitude of post-6 Ma uplift of Bidahochi samples assuming minimal zero elevation intercept of the lake water carbonate temperature (LCT) trend.

average of 30.7 ± 1.2°C, forming a cluster that is as tight as the Bidahochi Formation estimates (Figure 8). These samples thus record temperatures that on average are about 7°C warmer than the modern LCT curve. However, other than their being anomalously cool, there is no basis to exclude the two low temperature measurements from the lower basin data. Possible explanations that do not exclude any of the data are discussed in the following paragraphs.

[37] One hypothesis is that the four samples from the southernmost exposures of the Bouse Formation, all of which are currently only ~100 m above sea level, form a Gaussian population of measurements whose mean is the actual depositional temperature. If so the weighted average would be 27.3°C, about 4°C cooler than the weighted average of the remaining four lower basin samples, which today reside at elevations of 535 to 646 m. This temperature difference would imply substantial relative uplift of the northern sections from an initial position hundreds of meters below seal level. Given that the lower basin lakes were integrated into a throughgoing Colorado River drainage system soon after they formed [*Poulson and John*, 2003], and the rarity of tectonically inactive terrestrial basins lying below sea level, this hypothesis is highly unlikely.

[38] A second possibility is that the upstream samples are systematically reset and do not record depositional temperatures. There is no basis in the textures or oxygen isotope data to support this hypothesis, and *Spencer and Patchett* [1997] and *Poulson and John* [2003] noted that geologic evidence for diagenesis of Bouse carbonates is rare. Further, it would require resetting of six samples collected from four localities spanning a 300 km long reach of the lower basin to within a few degrees of each other. Although a possibility, we note that the large scatter in recorded temperatures of samples in units with evidence for resetting (e.g., Imperial Formation, 39°C, Westwater Formation, 47°C, Rim Gravels, 70°C) also suggests it is unlikely.

[39] A third possible explanation is that the cooler samples reflect the cooling of lake surface waters owing to either the influence of a marine climate or perhaps estuarine mixing. The pattern of decreasing ^{18}O of water values for the ancient samples versus distance from the coast at the time of deposition supports this hypothesis. The $\delta^{18}O$ of water is correlated with inland distance (r = 0.55), generally becoming more depleted in ^{18}O presumably due to the continentality effect [*Dansgaard*, 1964]. As noted in section 5.1, the two cool samples were obtained from the southernmost exposures of Bouse strata in the Blythe subbasin (Cibola area). The O isotopic values for the waters from which the Cibola samples precipitated plot slightly below oceanic $\delta^{18}O$ values (Figure 4a), suggesting a supply of precipitation from air masses that just left the ocean.

[40] Even if the Bouse in this area is nonmarine, the abundant marine fossils it contains also indicate that deposition likely occurred proximal to an ocean [*Spencer and Patchett*, 1997]. Upper Miocene strata of unambiguous marine origin occur in boreholes in the Yuma area about 50 km southeast of the Cibola samples, and marine waters may have been as close as 15 km from the sampled area (data reviewed by *Spencer and Patchett* [1997] and *Spencer et al.* [2008a]). Restoration of the Peninsular Ranges tectonic block 250 km southeastward along the southern San Andreas fault system since 6.5 Ma [*Oskin and Stock*, 2003] juxtaposes upper Miocene marine strata of Pacific affinity in the Los Angeles basin region to within a few tens of kilometers of the southern margin of the Blythe subbasin. This juxtaposition resulted in a hydrographic interconnection between the Los Angeles basin and the lower Colorado River drainage near 5 Ma, as demonstrated by distinctive fish species that are common to the two areas [*Spencer et al.*, 2008b]. Although the details of the paleogeography are not well constrained, collectively these data indicate that the lowermost Bouse basin was proximal to the open waters of the western Pacific.

[41] Such proximity to an ocean may have afforded substantial spring and summer cooling along the southern margin of the lake or estuary. Water at Earth's surface and in the atmosphere has a strong moderating effect on climate, depressing air temperatures near the coast relative to inland areas during warm months. For example, inland areas near sea level (e.g., Blythe, California) have late spring and summer temperatures on average 5°C warmer than along the coast of the Gulf of California (e.g., Puerto Peñasco, Mexico, Figure 9). An even more pronounced effect is observed for areas that are influenced by the relatively cold Pacific Ocean. Relative to Blythe, July air temperatures at Riverside, which is 60 km from the Pacific coast, are about 10°C cooler, and July temperatures at Ensenada, which is on the coast, are 15°C cooler (Figure 9). Such an air temperature effect could explain the cooler Cibola sample temperatures.

[42] Although we cannot rule out the possibility that the variation in temperature of the southernmost Bouse samples is related to unmodeled errors (e.g., due to seasonal rainfall patterns or the hypsometry of the lacustrine catchment), we

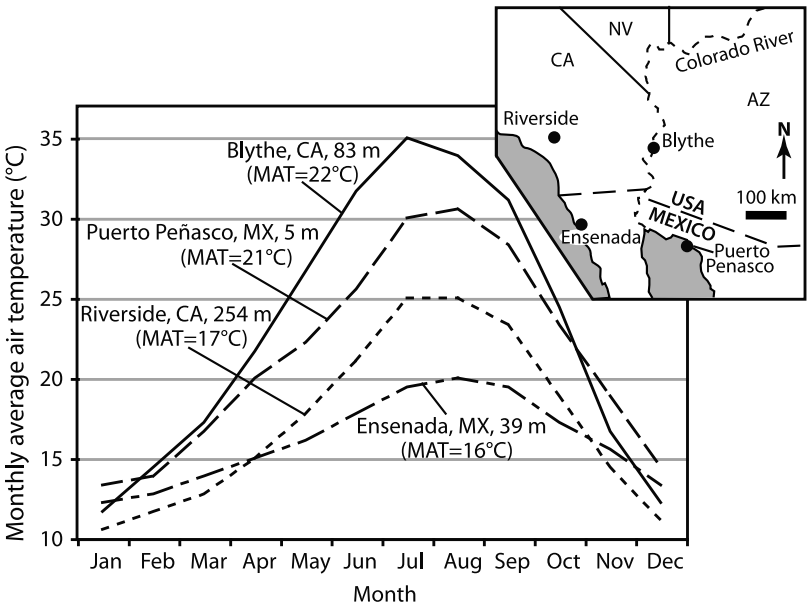

Figure 9. Mean monthly temperature curves for four cities in southwestern North America from the National Climatic Data Center (Weatherbase[SM]), showing the climatic influence of proximity to the marine waters of the Gulf of California (Puerto Peñasco) and Pacific Ocean (Riverside and Ensenada).

suggest that the variation records the influence of varying microclimates associated with proximity to the Pacific Ocean during deposition. In this interpretation, the warmest Cibola sample (i.e., 95BS10, collected immediately below the two cool samples at the same locality, which yielded a temperature of 30.5°C) would be most representative of the LCT zero elevation intercept, particularly given its similarity to lower basin temperatures recorded hundreds of kilometers inland from any potential influence of a marine climate. Excluding the two cool Bouse samples (unfilled circles, Figure 8), least squares linear regression through both upper and lower basin data plotted as a function of modern elevation yields a LCT lapse rate of 4.1°C/km with a zero elevation intercept of 32.1°C.

6.3. Relative Contribution of Uplift and Climate Change to Depositional Temperatures

[43] According to the interpretation presented above, the slope of the ancient LCT versus modern elevation trend is nearly identical to the modern LCT lapse rate of 4.2°C/km, suggesting that little if any change in elevation of the Bidahochi Formation is required to explain the data. The zero elevation intercept of the ancient trend is 7.7 ± 2.0°C (1σ) warmer than the modern trend, so this interpretation requires significant cooling due to climate change since late Miocene time.

[44] The magnitude of cooling since early Pliocene time indicated by the carbonate data is large, but plausible in light of other available paleotemperature proxy data. Although quantitative estimates of terrestrial paleotemperatures in the study area for this period are sparse, global climate in the Miocene is generally regarded to be several degrees warmer than today on the basis of stable isotopic records from benthic taxa in deep sea sediments [e.g., *Zachos et al.*, 2001]. These records may indicate up to 5°C of cooling of deep ocean waters since the Miocene-Pliocene transition [*Zachos et al.*, 2001, Figure 2]. Sea surface temperature (SST) records based on planktonic assemblages from the California margin [*Dowsett and Poore*, 2000] suggest that mean annual paleotemperatures off the coast of western North America were even warmer, indicating 7°C of cooling since Pliocene time. This large-magnitude temperature anomaly is corroborated by alkenone-based SST estimates from the same region [*Dekens et al.*, 2007]. Even if the magnitude of SST change off the coast of western North America was smaller than indicated by these studies, the magnitude of the SST anomaly might have been magnified in arid inland regions. As Figure 9 suggests, amplification of temperature variations in the arid continental interior may be especially pronounced during warm months, when carbonate precipitation in lakes is enhanced.

[45] If the offset between lake water temperatures estimated from modern and Miocene-Pliocene carbonates represents climatic cooling, in order for our data to be internally consistent it must be possible for large MAT changes to occur without significantly affecting the lapse rate. General circulation models of the atmosphere indicate that such changes in MAT should have little effect on low-latitude lapse rates [*Rind*, 1986]. Hence previous workers have applied modern lapse rates to paleoelevation reconstructions extending back as far as Eocene time in the southwestern United States [e.g., *Gregory and McIntosh*, 1996]. Modern temperature records for the Colorado Plateau region also suggest this approach is reasonable. As shown in Figure 6, seasonal variability in average monthly air temperature highs recorded by Arizona weather stations from 1971 to 2000 is greater than 20°C – far in excess of the inferred magnitude of cooling since 6 Ma. Yet

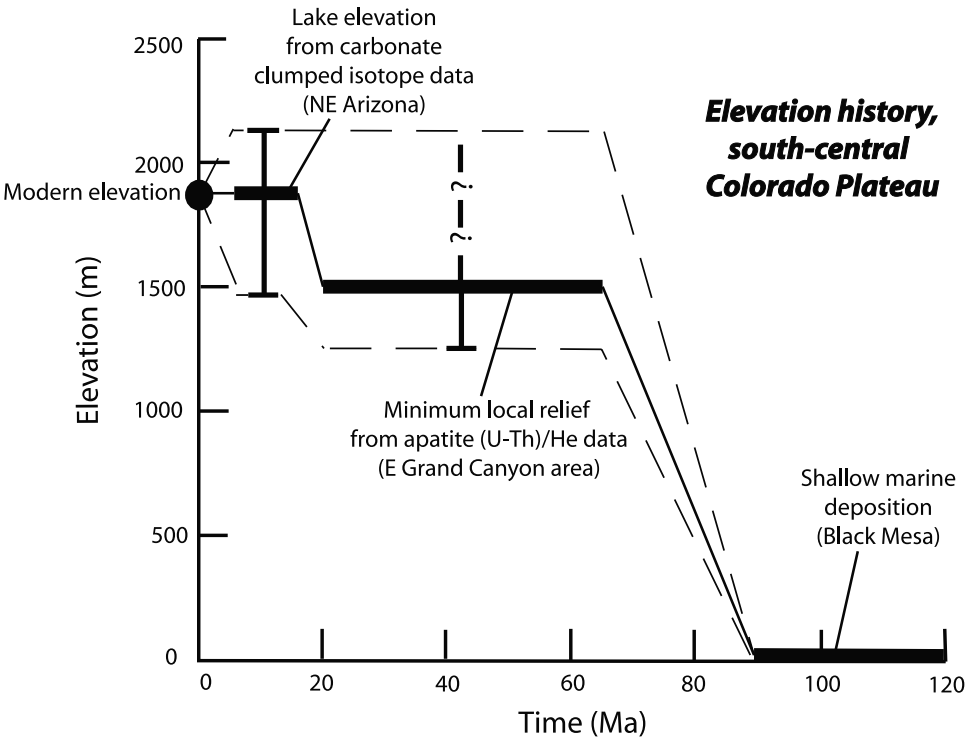

Figure 10. Plot showing elevation history of the southern interior of the Colorado Plateau based on the age of marine deposition [*Nations*, 1989], local relief inferred from (U-Th)/He dating [*Flowers et al.*, 2008], and lake elevation of the Bidahochi Formation (this study).

the lapse rate varies by less than 1°C throughout the year, providing strong evidence that even large MAT variations due to climate change would not cause significant changes in lapse rate. Given the likely stability of the MAT lapse rate, we presume that both the LST and LCT lapse rates were similar to that of today.

[46] Atmospheric lapse rates in the lower few kilometers of the troposphere are primarily sensitive to latitude and moisture content of the atmosphere [e.g., *Schneider*, 2007]. The lowest MAT lapse rates observed on Earth today, on the order of 3–4°C/km, are generally characteristic of humid, tropical regions [*Meyer*, 1986; *Schneider*, 2007, Figure 3.1]. Thus by analogy with modern climates, the ~6–8°C/km MAT lapse rates observed for the southwestern United States [*Meyer*, 1992] could have been a factor of two lower during the Miocene, if either the latitude or the relative humidity of the Colorado Plateau region at that time were substantially different from today. However, the average polar wander path for southwestern North America shows little latitude change since middle Miocene time [*Gripp and Gordon*, 2002]. Moreover, widespread deposition of evaporites in middle and late Miocene time in the southwestern United States [e.g., *Faulds et al.*, 2001] and other paleoenvironmental indicators [*Cather et al.*, 2008] suggest that the southwestern United States has generally been arid to semiarid since Oligocene time, further pointing to long-term stability of the MAT lapse rate.

[47] Given these observations, and our inference of marine influence on lake surface temperatures in the southernmost part of the Bouse basin, the recorded temperatures support the "null hypothesis" of little or no elevation change of the southern interior of the Colorado Plateau since 16 Ma, with 7.7 ± 2.0°C cooling in MAT of the southwestern interior since 6 Ma. The uncertainty in the modern LCT lapse rate from the data in Figure 3 is ± 0.6°C/km [*York*, 1968]. If we assume that the intercept of the lapse rate curve shifts 7.7°C, a 15% error in the LCT lapse rate, and a zero elevation intercept for the ancient carbonate trend of 32.1 ± 0.8°C, would be permissive of as much as 450 m of uplift of the plateau interior (Figure 8), or a Miocene elevation of ~1450 m for the Bidahochi basin. However, the data are equally consistent with 250 m of subsidence of the plateau since 6 Ma. The data thus permit a few hundred meters of elevation change of the southern plateau since 6 Ma, but do not support kilometer-scale changes (Figure 10).

7. Conclusions

[48] Our results bear on several important issues pertaining to the application of clumped isotope thermometry to problems in landscape evolution, and on paleoclimate and the tectonic evolution of the Colorado Plateau. First, Δ_{47} analysis of modern lake carbonates from 350 to 3300 m above sea level in the southwestern United States yields temperature estimates that are consistent with depositional conditions in the bodies of water from which they were collected, which are strongly elevation dependent. Although extensive additional limnological, conventional stable isotope, and clumped isotope work is needed to characterize Holocene variability in LCT lapse rates, this result based on

our preliminary data set suggests that ancient terrestrial carbonates also may record elevation-dependent depositional temperatures and therefore provide a robust paleoaltimetry proxy. Analysis of Tertiary carbonates from the Colorado Plateau region reveals that a wide variety of terrestrial carbonates record reasonable depositional temperatures and $\delta^{18}O$ values, provided they were never deeply buried. Although fossils appear to be susceptible to resetting, careful screening can help identify primary material for analysis [*Came et al.*, 2007].

[49] The results also underscore the importance of accounting for climate change when making estimates of paleoelevation with this technique. In particular, an accurate estimate of the contemporaneous zero elevation intercept of the LCT trend is crucial to demonstrating any changes (or lack thereof) in elevation of inland regions. Our results suggest that the zero elevation intercept may be difficult to measure, especially in situations where the only deposits demonstrably near sea level are either marine or proximal to an ocean. In this study, the consistency of temperatures recorded in the lower Colorado River basin samples, and the preservation of low-elevation deposits well inland from any potential marine influence, was critical to estimating the paleoelevation of the Bidahochi deposits. Nevertheless, future work involving a complete characterization of modern LCT variability and comparison of modern and ancient lacustrine systems including the Bouse depositional environment [e.g., *Spencer and Patchett*, 1997; *Poulson and John*, 2003] are needed to evaluate this interpretation.

[50] In addition to the zero elevation intercept, estimating the LCT lapse rate is also important. We determined the slope for modern deposits and inferred that the lapse rate in the past was similar to that of today. This interpretation appears reasonable, given the lack of major changes in latitude and general aridity of the region since Oligocene time. Although globally MAT lapse rates vary by nearly a factor of two, it is not yet clear whether the same is true of the LCT lapse rates, which depend on a complex combination of factors including air temperature, local hydrology, seasonality of precipitation, seasonal stratification in lakes, and carbonate saturation conditions that vary with season and water depth. The degree to which MAT lapse rates influence the LCT lapse rate will require an inventory of modern LCT lapse rates that sample a range of latitudes and atmospheric moisture levels.

[51] The primary implication of this study for the elevation history of the Colorado Plateau is that the results are consistent with the suggestion of *Flowers et al.* [2008] that the eastern Grand Canyon region had kilometer-scale local topographic relief similar to that of today from about 65 to 20 Ma, which requires a minimum elevation of upland areas in excess of this amount. Our data and those of *Flowers et al.* [2008] are permissive of up to several hundred meters of late Tertiary uplift. However, they do not require it, and also are consistent with the hypothesis of several hundred meters of late Tertiary subsidence of the southern plateau. Both data sets are inconsistent with an uplift estimate of 1100 m based on vesicular basalt paleoaltimetery on the 2 Ma Springerville basalt, which unconformably overlies the southern portion of the Bidahochi basin near the southern rim of the plateau [*Sahagian et al.*, 2002, 2003].

[52] If we have interpreted the data correctly, then most of the uplift of the south-central portion of the Colorado Plateau occurred during Late Cretaceous/earliest Tertiary time (Figure 10), favoring uplift mechanisms such as crustal thickening by lateral flow of deep crust [*McQuarrie and Chase*, 2000], hydration of the mantle lithosphere due to volatile flux from a newly arrived Laramide flat slab [*Humphreys et al.*, 2003], or dynamic topography associated with slab foundering [*Liu and Gurnis*, 2008]. We are careful to point out that our estimate of paleoelevation may not apply to the northern part of the plateau. Unlike the study region, the northern and western part of the plateau was a major lacustrine depocenter in Paleocene through middle Eocene time, accumulating some 1000 to 3000 m of sediment [e.g., *Hintze*, 1988]. Assessment of whether this depocenter was a lowland near sea level surrounded by 2000+ m Laramide uplands, or a high interior basin only slightly lower than the Laramide uplands, must await paleoelevation studies of these deposits. Whatever the origin of Laramide uplift, the data do not support explanations that ascribe most plateau uplift to late Eocene or younger (~40 to 0 Ma) disposal of either Farallon or North American mantle lithosphere. Although such events may have affected lithospheric buoyancy, they appear not to have been as significant as Late Cretaceous/earliest Tertiary events.

[53] **Acknowledgments.** This research was supported by National Science Foundation grants EAR-0610115 and EAR-0810824 and the Division of Geological and Planetary Sciences at the California Institute of Technology. This manuscript benefited from discussions with Gerard Roe and Tapio Schneider and was improved by thoughtful reviews by Brian Currie, Andreas Mulch, and Paul Kapp. We thank Jon Patchett, Dick Young, and Lesleigh Anderson, who provided many of the samples for which we report data, and Geoff Huntington for assistance in the field.

References

Affek, H., and J. M. Eiler (2006), Abundance of mass 47 CO_2 in urban air, car exhaust, and human breath, *Geochim. Cosmochim. Acta*, *67*, 1129–1143.

Axelrod, D. I. (1966), The Eocene Copper Basin flora of northeastern Nevada, *Univ. Calif. Publ. Geol. Sci.*, *59*, 1–125.

Beard, L. S. (1996), Paleogeography of the Horse Spring Formation in relation to the Lake Mead fault system, Virgin Mountains, Nevada and Arizona, in *Reconstructing the History of Basin and Range Extension Using Sedimentology and Stratigraphy*, *Geol. Soc. Am. Spec. Pap.*, vol. 303, edited by K. K. Beratan, pp. 27–60, Geol. Surv. of Am., Boulder, Colo.

Beus, S. S., and G. H. Billingsley (1989), Paleozoic strata of the Grand Canyon, Arizona, in *Geology of Grand Canyon, Northern Arizona (With Colorado River Guides): Lees Ferry to Pierce Ferry, Arizona*, edited by D. P. Elston, G. H. Billingsley, and R. A. Young, pp. 122–127, AGU, Washington, D. C.

Bird, P. (1979), Continental delamination and the Colorado Plateau, *J. Geophys. Res.*, *84*, 7561–7571.

Buising, A. V., and K. K. Beratan (1993), Preliminary stratigraphic reevaluation of upper Tertiary units, Osborne Wash area, La Paz county, Arizona, *U.S. Geol. Surv. Bull.*, *2053*, 159–163.

Came, R. E., J. M. Eiler, J. Veizer, K. Azmy, U. Brand, and C. R. Weidman (2007), Coupling of surface temperatures and atmospheric CO_2 concentrations during the Palaeozoic era, *Nature*, *449*, 198–202, doi:10.1038/nature06085.

Cather, S. M., S. D. Connell, R. M. Chamberlin, W. C. McIntosh, G. E. Jones, A. R. Potochnik, S. G. Lucas, and P. S. Johnson (2008), The Chuska erg: Paleogeomorphic and paleoclimatic implications of an Oligocene sand sea on the Colorado Plateau,

Geol. Soc. Am. Bull., *120*, 13–33, doi:10.1130/B26081.1.

Chamberlain, C. P., and M. A. Poage (2000), Reconstructing the paleotopography of mountain belts from the isotopic composition of authigenic minerals, *Geology*, *28*, 115–118, doi:10.1130/0091-7613(2000)28<115:RTPOMB>2.0.CO;2.

Dallegge, T. A. (1999), Correlation and chronology of the Miocene-Pliocene Bidahochi Formation, Navajo and Hopi Nations, northeastern Arizona, M.Sc. thesis, 304 pp., North. Ariz. Univ., Flagstaff, Ariz.

Dallegge, T. A., M. H. Y. Ort, W. C. McIntosh, and M. E. Perkins (2001), Age and depositional basin morphology of the Bidahochi Formation and implications for the ancestral Upper Colorado River, in *Colorado River: Origin and Evolution*, edited by R. A. Young and E. E. Spamer, pp. 47–52, Grand Canyon Assoc., Grand Canyon, Ariz.

Dansgaard, W. (1964), Stable isotopes in precipitation, *Tellus*, *16*, 436–468.

de Groot, P. A. (2009), *Handbook of Stable Isotope Analytical Techniques*, vol. 2, 284 pp., Elsevier, Amsterdam.

Dekens, P. S., A. C. Ravelo, and M. D. McCarthy (2007), Warm upwelling regions in the Pliocene warm period, *Paleoceanography*, *22*, PA3211, doi:10.1029/2006PA001394.

Dettman, D. L., and K. C. Lohmann (2000), Oxygen isotopic evidence for high-altitude snow in the Laramide Rocky Mountains of North America during Late Cretaceous and Paleogene, *Geology*, *28*, 243–246, doi:10.1130/0091-7613(2000)28<243:OIEFHS>2.0.CO;2.

Dillon, J. T., and P. L. Ehlig (1993), Displacement on the southern San Andreas fault, in *The San Andreas Fault System: Displacement, Palinspastic Reconstruction, and Geologic Evolution*, edited by R. E. Powell, R. J. Weldon II, and J. C. Matti, pp. 199–216, Geol. Soc. of Am., Boulder, Colo.

Dorsey, B. J., A. Fluette, K. McDougall, B. A. Housen, S. U. Janecke, G. J. Axen, and C. R. Shirvell (2007), Chronology of Miocene-Pliocene deposits at Split Mountain Gorge, southern California: A record of regional tectonics and Colorado River evolution, *Geology*, *35*, 57–60, doi:10.1130/G23139A.1.

Dowsett, H. J., and R. Z. Poore (2000), Data report: Pliocene planktic foraminifers from the California margin: Site 1021, *Proc. Ocean Drill. Program Sci. Results*, *167*, 115–117.

Duston, N. M., R. Owen, and B. H. Wilkinson (1986), Water chemistry and sedimentological observations in Littlefield Lake, Michigan: Implications for lacustrine marl deposition, *Environ. Geol. Water Sci.*, *8*, 229–236, doi:10.1007/BF02524950.

Effler, S. W., H. Greer, M. G. Perkins, S. D. Field, and E. Mills (1987), Calcium carbonate precipitation and transparency in lakes: A case study, *J. Environ. Eng.*, *113*, 124–133, doi:10.1061/(ASCE)0733-9372(1987)113:1(124).

Eiler, J. M. (2007), "Clumped-isotope" geochemistry-The study of naturally occurring multiply substituted isotopologues, *Earth Planet. Sci. Lett.*, *262*, 309–327, doi:10.1016/j.epsl.2007.08.020.

Eiler, J. M., and E. Schauble (2004), $^{18}O^{13}C^{16}O$ in Earth's atmosphere, *Geochim. Cosmochim. Acta*, *68*, 4767–4777, doi:10.1016/j.gca.2004.05.035.

Elston, D. P., and R. A. Young (1991), Cretaceous-Eocene (Laramide) landscape development and Oligocene-Pliocene drainage reorganization of transition zone and Colorado Plateau, Arizona, *J. Geophys. Res.*, *96*, 12,389–12,406, doi:10.1029/90JB01978.

Faulds, J. E., M. A. Wallace, L. A. Gonzales, and M. T. Heizler (2001), Depositional environment and paleogeographic implications of the late Miocene Hualapai Limestone, northwestern Arizona, in *Colorado River: Origin and Evolution*, edited by in R. A. Young and E. E. Spamer, pp. 81–88, Grand Canyon Assoc., Grand Canyon, Ariz.

Flowers, R. M., B. Wernicke, and K. A. Farley (2008), Unroofing, incision and uplift history of the southwestern Colorado Plateau from (U-Th)/He apatite thermochronometry, *Geol. Soc. Am. Bull.*, *120*, 571–587, doi:10.1130/B26231.1.

Forest, C. E., J. A. Wolfe, P. Molnar, and K. A. Emanuel (1999), Paleoaltimetry incorporating atmospheric physics and botanical estimates of paleoclimate, *Geol. Soc. Am. Bull.*, *111*, 497–511, doi:10.1130/0016-7606(1999)111<0497:PIAPAB>2.3.CO;2.

Garzione, C. N., D. L. Dettman, J. Quade, P. G. DeCelles, and R. F. Butler (2000), High times on the Tibetan Plateau: Paleoelevation of the Thakkhola Graben, Nepal, *Geology*, *28*, 339–342, doi:10.1130/0091-7613(2000)28<339:HTOTTP>2.0.CO;2.

Ghosh, P., J. Adkins, H. Affek, B. Balta, W. Guo, E. Schauble, D. Schrag, and J. Eiler (2006a), ^{13}C-^{18}O bonds in carbonate minerals: A new kind of paleothermometer, *Geochim. Cosmochim. Acta*, *70*, 1439–1456, doi:10.1016/j.gca.2005.11.014.

Ghosh, P., C. Garzione, and J. M. Eiler (2006b), Rapid uplift of the Altiplano revealed through ^{13}C-^{18}O bonds in paleosol carbonates, *Science*, *311*, 511–515, doi:10.1126/science.1119365.

Gregory, K. M., and C. G. Chase (1992), Tectonic significance of paleobotanically estimated climate and altitude of the late Eocene erosion surface, Colorado, *Geology*, *20*, 581–585, doi:10.1130/0091-7613(1992)020<0581:TSOPEC>2.3.CO;2.

Gregory, K. M., and W. C. McIntosh (1996), Paleoclimate and paleoelevation of the Oligocene Pitch-Pinnacle flora, Sawatch Range, Colorado, *Geol. Soc. Am. Bull.*, *108*, 545–561, doi:10.1130/0016-7606(1996)108<0545:PAPOTO>2.3.CO;2.

Gripp, A. E., and R. G. Gordon (2002), Young tracks of hotspots and current plate velocities, *Geophys. J. Int.*, *150*, 321–361, doi:10.1046/j.1365-246X.2002.01627.x.

Gross, E. L., P. J. Patchett, T. A. Dallegge, and J. E. Spencer (2001), The Colorado River System and Neogene sedimentary formations along its course: Apparent Sr isotopic connections, *J. Geol.*, *109*, 449–461, doi:10.1086/320793.

Guay, B. E., C. J. Estoe, R. Bassett, and A. Long (2006), Identifying sources of groundwater in the lower Colorado River valley, USA, with $\delta^{18}O$, δD, and ^{3}H: Implications for river water accounting, *Hydrogeol. J.*, *14*, 146–158, doi:10.1007/s10040-004-0334-4.

Guo, W., and J. Eiler (2007), Temperatures of aqueous alteration and evidence for methane generation on the parent bodies of the CM chondrites, *Geochim. Cosmochim. Acta*, *71*, 5565–5575, doi:10.1016/j.gca.2007.07.029.

Hintze, L. F. (1988), *Geologic History of Utah: A Field Guide to Utah's Rocks*, vol. 7, 193 pp., Brigham Young Univ., Provo, Utah.

Hintze, L. F (1993), *Geologic History of Utah*, 202 pp., Brigham Young Univ., Provo, Utah.

Holm, R. F. (2001), Cenozoic paleogeography of the central Mogollon Rim, southern Colorado Plateau region, Arizona, revealed by Tertiary gravel deposits, Oligocene to Pleistocene lava flows, and incised streams, *Geol. Soc. Am. Bull.*, *113*, 1467–1485, doi:10.1130/0016-7606(2001)113<1467:CPOTCM>2.0.CO;2.

Horton, T. W., and C. Chamberlain (2006), Stable isotopic evidence for Neogene surface downdrop in the central Basin and Range Province, *Geol. Soc. Am. Bull.*, *118*, 475–490, doi:10.1130/B25808.

Horton, T. W., D. J. Sjostrom, M. J. Abruzzese, M. A. Poage, J. R. Waldbauer, M. Hren, J. L. Wooden, and C. P. Chamberlain (2004), Spatial and temporal variation of Cenozoic surface elevation in the Great Basin and Sierra Nevada, *Am. J. Sci.*, *304*, 862–888, doi:10.2475/ajs.304.10.862.

House, P. K., P. A. Pearthree, and M. E. Perkins (2008), Stratigraphic evidence for the role of lake spillover in the inception of the lower Colorado River in southern Nevada and western Arizona, in *Late Cenozoic Drainage History of the Southwestern Great Basin and Lower Colorado River Region: Geologic and Biotic Perspectives*, *Geol. Soc. Am. Spec. Pap.*, vol. 439, edited by M. C. Reheis, R. Hershler, and D. M. Miller, pp. 335–353, doi:10.1130/2008.2439(15), Geol. Soc. of Am., Boulder, Colo.

Humphreys, E. D. (1995), Post-Laramide removal of the Farallon slab, western United States, *Geology*, *23*, 987–990, doi:10.1130/0091-7613(1995)023<0987:PLROTF>2.3.CO;2.

Humphreys, E. D., E. Hessler, K. Dueker, C. L. Farmer, E. A. Erslev, and T. Atwater (2003), How Laramide-age hydration of North American lithosphere by the Farallon slap controlled subsequent activity in the western United States, *Int. Geol. Rev.*, *45*, 575–595, doi:10.2747/0020-6814.45.7.575.

Hunt, C. B. (1956), Cenozoic geology of the Colorado Plateau, *U.S. Geol. Surv. Prof. Pap.*, *279*, 1–99.

Huntington, K. W., et al. (2009), Methods and limitations of "clumped" CO_2 isotope ($\Delta 47$) analysis by gas-source isotope-ratio mass spectrometry, *J. Mass Spectrom.*, *44*, 1318–1329.

Ingle, J. C., Jr. (1973), Neogene marine history of the Gulf of California: Foraminiferal evidence, *Geol. Soc. Am. Abstr. Programs*, *5*, 62.

Ingle, J. C., Jr. (1974), Paleobathymetric history of Neogene marine sediments, southern Gulf of California, in *Geology of the Peninsular California: American Association of Petroleum Geologists Guidebook*, edited by G. Gastil and J. Lillegraven, pp. 121–138, Am. Assoc. of Petrol. Geol., Bakersfield, Calif.

Johnson, N. M., C. B. Officer, N. D. Opdyke, G. D. Woodard, P. K. Zeitler, and E. H. Lindsay (1983), Rates of late Cenozoic tectonism in the Vallecito-Fish Creek basin, western Imperial Valley, *Calif. Geol.*, *11*, 664–667.

Jones, C. G., G. L. Farmer, and J. R. Unruh (2004), Tectonics of Pliocene removal of lithosphere of the Sierra Nevada, California, Geol. *Soc. Am. Bull.*, *116*, 1408–1422, doi:10.1130/B25397.1.

Karlstrom, K. E., R. S. Crow, L. Peters, W. McIntosh, J. Raucci, L. J. Crossey, P. Umhoefer, and N. Dunbar (2007), $^{40}Ar/^{39}Ar$ and field studies of Quaternary basalts in Grand Canyon and model for carving Grand Canyon: Quantifying the interaction of river incision and normal faulting across the western edge of the Colorado Plateau, *Geol. Soc. Am. Bull.*, *199* (11–12), 1283–1312.

Kerr, D. R., and S. M. Kidwell (1991), Late Cenozoic sedimentation and tectonics, western Salton Trough, California, in *Geological Excursions in Southern California and Mexico*, edited by M. J. Walawender and B. B. Hanan, pp. 397–416, San Diego State Univ., San Diego, Calif.

Kim, S.-T., and J. R. O'Neil (1997), Equilibrium and nonequilibrium oxygen isotope effects in synthetic carbonates, *Geochim. Cosmochim. Acta*, *61*, 3461–3475, doi:10.1016/S0016-7037(97)00169-5.

Lamb, M., P. J. Umhoefer, E. Anderson, L. S. Beard, T. Hickson, and K. L. Martin (2005), Development of Miocene faults and basins in the Lake Mead region: A tribute to Ernie Anderson and a review of new research on basins, in *Interior Western United States*, *Geol. Soc. Am. Field Guide*, vol. 6, edited by J. Pederson and C. M. Dehler, pp. 389–418, Geol. Soc. of Am., Boulder, Colo.

Libarkin, J. C., and C. G. Chase (2003), Timing of Colorado Plateau uplift: Initial constraints from vesicular basalt-derived paleoelevaions: Comment and Reply: Comment, *Geology*, *31*, 191–192, doi:10.1130/0091-7613(2003)031<0191:TOCPUI>2.0.CO;2.

Liu, L., and M. Gurnis (2008), Simultaneous inversion of mantle properties and initial conditions using an adjoint of mantle convection, *J. Geophys. Res.*, *113*, B08405, doi:10.1029/2008JB005594.

Love, D. W. (1989), Bidahochi Formation: An interpretive summary, in *Southwestern Colorado Plateau: 40th Field Conference Guidebook*, edited by O. J. Anderson, pp. 273–280, N. M. Geol. Soc., Socorro, N. M.

Manabe, S., and T. B. Terpstra (1974), The effects of mountains on the general circulation of the atmosphere as identified by numerical experiments, *J. Atmos. Sci.*, *31*, 3–42, doi:10.1175/1520-0469(1974)031<0003:TEOMOT>2.0.CO;2.

McCrea, J. M. (1950), On the isotopic chemistry of carbonates and a paleotemperature scale, *J. Chem. Phys.*, *18*, 849–857, doi:10.1063/1.1747785.

McDougall, K. (2008), Late Neogene marine incursions and the ancestral Gulf of California, in *Late Cenozoic Drainage History of the Southwestern Great Basin and Lower Colorado River Region: Geologic and Biotic Perspectives*, *Geol. Soc. Am. Spec. Pap.*, vol. 439, edited by M. C. Reheis, R. Hershler, and D. M. Miller, pp. 355–373, doi:10.1130/2008.2439(16), Geol. Soc. of Am., Boulder, Colo.

McGetchin, T. R., K. C. Burk, G. A. Thompson, and R. A. Young (1980), Mode and mechanism of plateau uplifts, in *Dynamics of Plate Interiors*, *Geodyn. Ser.*, vol. 1, edited by A.W. Bally et al., pp. 99–110, AGU, Washington, D. C.

McQuarrie, N., and C. G. Chase (2000), Raising the Colorado Plateau, *Geology*, *28*, 91–94, doi:10.1130/0091-7613(2000)028<0091:RTCP>2.0.CO;2.

Meyer, H. W. (1986), An evaluation of the methods for estimating paleoaltitudes using Tertiary floras from the Rio Grande rift vicinity, New Mexico and Colorado, Ph.D. dissertation, 217 pp., Univ. of Calif., Berkeley, Calif.

Meyer, H. W. (1992), Lapse rates and other variables applied to estimating paleoaltitudes from fossil floras, *Palaeogeogr. Palaeoclimatol. Palaeoecol.*, *99*, 71–99, doi:10.1016/0031-0182(92)90008-S.

Molnar, P., and P. England (1990), Late Cenozoic uplift of mountain ranges and global climate change: Chicken or egg?, *Nature*, *346*, 29–34, doi:10.1038/346029a0.

Molnar, P., P. England, and J. Martinod (1993), Mantle dynamics, uplift of the Tibetan Plateau, and the Indian monsoon, *Rev. Geophys.*, *31*, 357–396, doi:10.1029/93RG02030.

Morgan, P., and C. A. Swanberg (1985), On the Cenozoic uplift and tectonic stability of the Colorado Plateau, *J. Geodyn.*, *3*, 39–63, doi:10.1016/0264-3707(85)90021-3.

Mosbrugger, V. (1999), The nearest living relative method, in *Fossil Plants and Spores: Modern Techniques*, edited by T. P. Jones and N. P. Rowe, pp. 261–265, Geol. Soc. of London, London.

Mulch, A., S. A. Graham, and C. P. Chamberlain (2006), Hydrogen isotopes in Eocene river gravels and paleoelevation of the Sierra Nevada, *Science*, *313*, 87–89, doi:10.1126/science.1125986.

Mulch, A., C. Teyssier, M. A. Cosca, and C. P. Chamberlain (2007), Stable isotope paleoaltimetry of Eocene core complexes in the North American Cordillera, *Tectonics*, *26*, TC4001, doi:10.1029/2006TC001995.

Mulch, A., A. M. Sarna-Wojcicki, M. E. Perkins, and C. P. Chamberlain (2008), A Miocene to Pleistocene climate and elevation record of the Sierra Nevada (California), *Proc. Natl. Acad. Sci. U. S. A.*, *105*, 6819–6824, doi:10.1073/pnas.0708811105.

Nations, J. D. (1989), Cretaceous history of northeastern and east-central Arizona, in *Geology of Arizona*, edited by J. P. Jenny and S. J. Reynolds, pp. 435–446, Ariz. Geol. Soc., Tucson, Ariz.

Oskin, M., and J. Stock (2003), Pacific-North America plate motion and opening of the Upper Delfín basin, northern Gulf of California, Mexico, *Geol. Soc. Am. Bull.*, *115*, 1173–1190, doi:10.1130/B25154.1.

Parsons, T., and J. McCarthy (1995), The active southwest margin of the Colorado Plateau: Uplift of mantle origin, *Geol. Soc. Am. Bull.*, *107*, 139–147, doi:10.1130/0016-7606(1995)107<0139:TASMOT>2.3.CO;2.

Pederson, J., K. Karlstrom, W. Sharp, and W. McIntosh (2002), Differential incision of the Grand Canyon related to Quaternary faulting—Constraints from U-series and Ar/Ar dating, *Geology*, *30*, 739–742, doi:10.1130/0091-7613(2002)030<0739:DIOTGC>2.0.CO;2.

Peirce, H.W., P.E. Damon, and M. Shafiqullah (1979), An Oligocene (?) Colorado Plateau edge in Arizona, *Tectonophysics*, *61*, 1–24, doi:10.1016/0040-1951(79)90289-0.

Poage, M. A., and C. P. Chamberlain (2001), Empirical relationships between elevation and the stable isotope composition of precipitation: Considerations for studies of paleoelevation change, *Am. J. Sci.*, *301*, 1–15, doi:10.2475/ajs.301.1.1.

Poage, M. A., and C. Chamberlain (2002), Stable isotopic evidence for a pre-Middle Miocene rain shadow in the western Basin and Range: Implications for the paleotopography of the Sierra Nevada, *Tectonics*, *21*(4), 1034, doi:10.1029/2001TC001303.

Potochnik, A. R. (1989), Depositional style and tectonic implications of the Mogollon Rim Formation (Eocene), east-central Arizona, in *Southeastern Colorado Plateau: 40th Field Conference Guidebook*, edited by O. J. Anderson, pp.107–118, N. M. Geol. Soc., Socorro, N. M.

Potochnik, A. R. (2001), Paleogeomorphic evolution of the Salt River Region: Implications for Cretaceous-Laramide inheritance for ancestral Colorado River drainage, in *Colorado River: Origin and Evolution*, edited by R. A. Young and E. E. Spamer, pp. 17–24, Grand Canyon Assoc., Grand Canyon, Ariz.

Poulson, S. R., and B. E. John (2003), Stable isotope and trace element geochemistry of the basal Bouse Formation carbonate, southwestern United States: Implications for the Pliocene uplift history of the Colorado Plateau, *Geol. Soc. Am. Bull.*, *115*, 434–444, doi:10.1130/0016-606(2003)1115<0434:SIATEG>1132.1130.CO;1132.

Quade, J., C. Garzione, and J. Eiler (2007), Paleoelevation reconstruction using pedogenic carbonates, *Rev. Mineral. Geochem.*, *66*, 53–87, doi:10.2138/rmg.2007.66.3.

Repenning, C. A., and J. H. Irwin (1954), Bidahochi Formation of Arizona and New Mexico, *Am. Assoc. Pet. Geol. Bull.*, *38*, 1821–1826.

Rind, D. (1986), The dynamics of warm and cold climates, *J. Atmos. Sci.*, *43*, 3–25.

Rowley, D. B., and C. N. Garzione (2007), Stable isotope-based paleoaltimetry, *Annu. Rev. Earth Planet. Sci.*, *35*, 463–508, doi:10.1146/annurev.earth.35.031306.140155.

Roy, M., J. K. MacCarthy, and J. Selverstone (2005), Upper mantle structure beneath the eastern Colorado Plateau and Rio Grande rift revealed by Bouguer gravity, seismic velocities, and xenolith data, *Geochem. Geophys. Geosyst.*, *6*, Q10007, doi:10.1029/2005GC001008.

Ruddiman, W. F., and J. E. Kutzbach (1989), Forcing of the late Cenozoic northern hemisphere climate by plateau uplift in southeast Asia and the American southwest, *J. Geophys. Res.*, *94*, 18,409–18,427, doi:10.1029/JD094iD15p18409.

Sahagian, D., A. Proussevitch, and W. Carlson (2002), Timing of Colorado Plateau uplift: Initial constraints from vesicular basalt-derived paleoelevations, Geology, 30, 807–810, doi:10.1130/0091-7613(2002)030<0807:TOCPUI>2.0.CO;2.

Sahagian, D., A. Proussevitch, and W. Carlson (2003), Analysis of vesicular basalts and lava emplacement processes for application as a paleobarometer/paleoaltimeter: A reply, *Geology*, *111*, 502–504, doi:10.1086/375278.

Schauble, E. A., P. Ghosh, and J. M. Eiler (2006), Preferential formation of ^{13}C-^{18}O bonds in carbonate minerals, estimated using first-principles lattice dynamics, *Geochim. Cosmochim. Acta*, *70*, 2510–2529, doi:10.1016/j.gca.2006.02.011.

Schneider, T. (2007), Thermal stratification of the extratropical troposphere, in *The Global Circulation of the Atmosphere*, edited by T. Schneider and A. H. Sobel, pp. 47–77, Princeton Univ. Press, Princeton, N. J.

Spencer, J. E. (1996), Uplift of the Colorado Plateau due to lithospheric attenuation during Laramide low-angle subduction, *J. Geophys. Res.*, *101*, 13,595–13,609, doi:10.1029/96JB00818.

Spencer, J. E., and P. J. Patchett (1997), Sr isotope evidence for a lacustrine origin for the upper Miocene to Pliocene Bouse Formation, lower Colorado River trough, and implications for timing of Colorado Plateau uplift, *Geol. Soc. Am. Bull.*, *109*, 767–778, doi:10.1130/0016-7606(1997)109<0767:SIEFAL>2.3.CO;2.

Spencer, J. E., L. Peters, W. C. McIntosh, and P. J. Patchett (2001), $^{40}Ar/^{39}Ar$ geochronology of the Hualapai Limestone and Bouse Formation and implications for the age of the lower Colorado River, in *Colorado River: Origin and Evolution*, edited by R. A. Young and E. E. Spamer, pp. 89–92, Grand Canyon Assoc., Grand Canyon, Ariz.

Spencer, J. E., P. A. Pearthree, and P. K. House (2008a), An evaluation of the evolution of the latest Miocene to earliest Pliocene Bouse lake system in the lower Colorado River Valley, southwestern USA, in *Late Cenozoic Drainage History of the Southwestern Great Basin and Lower Colorado River Region: Geologic and Biotic Perspectives*, *Geol. Soc. Am. Spec. Pap.*, vol. 439, edited by M. C. Reheis, R. Hershler, and D. M. Miller, pp. 375–390, doi:10.1130/2008.2439(17), Geol. Soc. of Am., Boulder, Colo.

Spencer, J. E., G. R. Smith, and T. E. Dowling (2008b), Middle to late Cenozoic geology, hydrography, and fish evolution in the American Southwest, in *Late Cenozoic Drainage History of the Southwestern Great Basin and Lower Colorado River Region: Geologic and Biotic Perspectives*, *Geol. Soc. Am. Spec. Pap.*, vol. 439, edited by M. C. Reheis, R. Hershler, and D. M. Miller, pp. 279–299, doi:10.1130/2008.2439(12), Geol. Soc. of Am., Boulder, Colo.

Stunm, W., and J. J. Morgan (1981), *Aquatic Chemistry: An Introduction Emphasizing Chemical Equilibria in Natural Waters*, 2nd ed., 780 pp., Wiley, New York.

Swart, P. K., S. J. Burns, and J. J. Leder (1991), Fractionation of the stable isotopes of oxygen and carbon in carbon dioxide during the reaction of calcite with phosphoric acid as a function of temperature and technique, *Chem. Geol. Isot. Geosci. Sect.*, *86*, 89–96, doi:10.1016/0168-9622(91)90055-2.

Thompson, G. A., and M. L. Zoback (1979), Regional geophysics of the Colorado Plateau, *Tectonophysics*, *61*, 149–181, doi:10.1016/0040-1951(79)90296-8.

Wallace, M. W., J. E. Faulds, and R. J. Brady (2005), Geologic map of the Meadview North Quadrangle, Arizona and Nevada, map, 22 pp., scale 1:24,000, Nev. Bur. of Mines and Geol., Reno, Nev.

Wang, Z., E. A. Schauble, and J. M. Eiler (2004), Equilibrium thermodynamics of multiply substituted isotopologues of molecular gases, *Geochim. Cosmochim. Acta*, *68*, 4779–4797, doi:10.1016/j.gca.2004.05.039.

Winker, C. D. (1987), Neogene stratigraphy of the Fish Creek-Vallecito section, southern California: Implications for early history of the northern Gulf of California and Colorado delta (San Andreas Fault), Ph.D. dissertation, 622 pp., Univ. of Arizona, Tucson, Ariz.

Winker, C. D., and S. M. Kidwell (1986), Paleocurrent evidence for lateral displacement of the Pliocene Colorado River delta by the San Andreas fault system, southeastern California, *Geology*, *14*, 788–791, doi:10.1130/0091-7613(1986)14<788:PEFLDO>2.0.CO;2.

Winterer, J. L. (1975), Biostratigraphy of Bouse Formation: A Pliocene Gulf of California deposit in California, Arizona, and Nevada, M.S. thesis, 132 pp., Calif. State Univ., Long Beach, Calif.

Wolfe, J. A., and D. M. Hopkins (1967), Climatic changes recorded by Tertiary land floras in northwestern North America, in *Tertiary Correlations and Climate Changes in the Pacific*, edited by H. Hatai, pp. 67–76, Sesaki, Sendai, Japan.

Wolfe, J. A., H. E. Schorn, C. E. Forest, and P. Molnar (1997), Paleobotanical evidence for high altitudes in Nevada during the Miocene, *Science*, *276*(5319), 1672–1675, doi:10.1126/science.276.5319.1672.

Wolfe, J. A., C. E. Forest, and P. Molnar (1998), Paleobotanical evidence of Eocene and Oligocene paleoaltitudes in midlatitude western North America, *Geol. Soc. Am. Bull.*, *110*, 664–678, doi:10.1130/0016-7606(1998)110<0664:PEOEAO>2.3.CO;2.

York, D. (1968), Least-squares fitting of a straight line with correlated errors, *Earth Planet. Sci. Lett.*, *5*, 320–324, doi:10.1016/S0012-821X(68)80059-7.

Young, R. A. (1989), Paleogene-Neogene deposits of western Grand Canyon, Arizona, in *Geology of Grand Canyon, Northern Arizona (With Colorado River Guides): Lees Ferry to Pierce Ferry, Arizona*, edited by D. P. Elston, G. H. Billingsley, and R. A. Young, pp. 166–173, AGU, Washington, D. C.

Young, R. A. (1999), Nomenclature and ages of late Cretaceous(?)-Tertiary strata in the Hualapai Plateau region, northwest Arizona, *U.S. Geol. Surv. Misc. Invest. Map*, *I-2554*.

Young, R. A. (2001), The Laramide-Paleogene history of the western Grand Canyon region: Setting the stage, in *Colorado River: Origin and Evolution*, edited by R. A. Young and E. E. Spamer, pp. 7–16, Grand Canyon Assoc., Grand Canyon, Ariz.

Zachos, J. C., M. Pagani, L. Sloan, E. Thomas, and K. Billups (2001), Trends, rhythms, and aberrations in global climate 65 Ma to Present, *Science*, *292*, 686–693, doi:10.1126/science.1059412.

Zandt, G., H. Gilbert, T. Owens, M. Ducea, J. Saleeby, and C. Jones (2004), Active foundering of a continental arc root beneath the southern Sierra Nevada in California, *Nature*, *431*, 41–46, doi:10.1038/nature02847.

J. M. Eiler and B. P. Wernicke, Division of Earth and Planetary Sciences, California Institute of Technology, Pasadena, CA 91125, USA.

K. W. Huntington, Department of Earth and Space Sciences, University of Washington, Seattle, WA 98195, USA. (kate1@u.washington.edu)